

Tidal evolution for any rheological model using a vectorial approach expressed in Hansen coefficients.

Alexandre C. M. Correia · Ema F. S. Valente

June 7, 2023

Abstract We revisit the two body problem, where one body can be deformed under the action of tides raised by the companion. Tidal deformation and consequent dissipation result in spin and orbital evolution of the system. In general, the equations of motion are derived from the tidal potential developed in Fourier series expressed in terms of Keplerian elliptical elements, so that the variation of dissipation with amplitude and frequency can be examined. However, this method introduces multiple index summations and some orbital elements depend on the chosen frame, which is prone to confusion and errors. Here, we develop the quadrupole tidal potential solely in a series of Hansen coefficients, which are widely used in celestial mechanics and depend just on the eccentricity. We derive the secular equations of motion in a vectorial formalism, which is frame independent and valid for any rheological model. We provide expressions for a single average over the mean anomaly and for an additional average over the argument of the pericentre. These equations are suitable to model the long-term evolution of a large variety of systems and configurations, from planet-satellite to stellar binaries. We also compute the tidal energy released inside the body for an arbitrary configuration of the system.

Keywords Extended Body Dynamics · Dissipative Forces · Stellar Systems · Planetary Systems · Natural Satellites · Rotation of Celestial Bodies

1 Introduction

Tidal effects arise when an extended body is placed in a differential gravitational field, such as the one generated by a point mass companion. For non-rigid bodies, each mass element adjusts to the equipotential surface, which gives rise to a global redistribution of mass known as tidal bulge. In the process, the friction inside the extended body introduces a delay between the initial perturbation and the maximal deformation. As a consequence, the companion exerts a torque on the tidal bulge of the extended body, which modifies its spin and the orbit.

The estimates for the tidal evolution of a body are based on a very general formulation of the tidal potential, initiated by [Darwin \(1879\)](#). Assuming a homogeneous body consisting of an

A. C. M. Correia
CFisUC, Departamento de Física, Universidade de Coimbra, 3004-516 Coimbra, Portugal
IMCCE, Observatoire de Paris, PSL Université, 77 Av. Denfert-Rochereau, 75014 Paris, France

E. F. S. Valente
CFisUC, Departamento de Física, Universidade de Coimbra, 3004-516 Coimbra, Portugal

incompressible fluid with constant viscosity, Darwin derived a tide-generated disturbing potential expanded into a Fourier series expressed in terms of elliptical elements. The equations of motion are then obtained using the Lagrange planetary equations (Darwin, 1880).

Kaula (1964) writes the tidal potential using Love numbers (Love, 1911). Each term of the Fourier series involves a Love number associated with the amplitude of the tide and a phase lag accounting for the non-instantaneous deformation of the body. This description is more general than Darwin's, because it makes no assumption on the rheology of the body (e.g., Efroimsky, 2012). Different rheologies have been proposed for satellites, rocky planets, giant gaseous or stars (e.g., Mignard, 1979; Ogilvie and Lin, 2004, 2007; Efroimsky and Lainey, 2007; Ferraz-Mello, 2013; Correia et al, 2014; Renaud and Henning, 2018), some because of their simplicity, others motivated by theoretical studies, laboratory experiments or geophysical measurements.

The description by Kaula also has a more compact and systematic form of the tidal potential, thus being more convenient for examining the tidal effects of varying conditions. However, sometimes there is an ambiguity in the interpretation of the frequencies involved in the phase lags (e.g., Efroimsky and Williams, 2009). Moreover, mistakes such as neglecting energy or momentum conservation considerations are more easily made. Indeed, Boué and Efroimsky (2019) have shown that additional terms need to be included owing to the conservation of the angular momentum and non-inertial frame considerations.

The classical expansion of the tidal potential in elliptical elements depends on the chosen frame and also introduces multiple index summations, which can lead to confusion and errors in the equations of motion. In the case of a linear constant time-lag model, which can be seen as a first order expansion of a viscoelastic rheology (Singer, 1968; Mignard, 1979), it has been shown that the equations of motion are more easily expressed in terms of angular momentum vectors (e.g., Correia, 2009; Correia et al, 2011). Therefore, in this paper we aim to also use these vectors for any rheological model that can be expressed in terms of Love numbers. This formalism is independent of the reference frame and allows to simply add the tidal contributions of multiple bodies in the system.

In Sect. 2, using the quadrupole tidal potential expanded in series of Hansen coefficients, we obtain the equations of motion using vectors and Love numbers. In Sect. 3 and Sect. 4, we average the equations of motion over the mean anomaly, and over the argument of the pericentre, respectively, which provide simpler expressions that are easily to implement and suitable for long-term evolution studies. In Sect. 5, we provide the equations of motion for the more simple planar case, and in Sect. 6, we explain how the equations of motion simplify for the linear constant time-lag model. Finally, we discuss our results in Sect. 7.

2 Two body problem with tides

We consider a system of two bodies with masses m_0 and m in a Keplerian orbit. The orbital angular momentum is given by (e.g., Murray and Dermott, 1999)

$$\mathbf{G} = \beta \sqrt{\mu a(1 - e^2)} \mathbf{k}, \quad (1)$$

where a is the semi-major axis, e is the eccentricity, $\beta = m_0 m / (m_0 + m)$, $\mu = \mathcal{G}(m_0 + m)$, \mathcal{G} is the gravitational constant, and \mathbf{k} is the unit vector along the direction of \mathbf{G} , which is normal to the orbit. The body with mass m_0 , named as ‘‘perturber’’, is a point mass object. The body with mass m , named as ‘‘central body’’, is an extended body and can be deformed under the action of tides. It rotates with angular velocity $\boldsymbol{\omega} = \omega \mathbf{s}$, where \mathbf{s} is the unit vector along the direction of the spin axis. The rotational angular momentum is given by

$$\mathbf{L} = C\boldsymbol{\omega} + \mathcal{I} \cdot \boldsymbol{\omega}, \quad (2)$$

where C is the moment of inertia of a sphere and

$$\mathcal{I} = \begin{bmatrix} I_{11} & I_{12} & I_{13} \\ I_{12} & I_{22} & I_{23} \\ I_{13} & I_{23} & I_{33} \end{bmatrix} \quad (3)$$

is the inertia tensor that accounts for the departure from the sphere. In the absence of the perturber, the central body is a perfect sphere, and so $\mathcal{I} = 0$. However, when the perturber is present, the central body is deformed, and \mathcal{I} can change. In this work we assume that the central body is incompressible, and thus $\text{tr}(\mathcal{I}) = I_{11} + I_{22} + I_{33} = 0$ (e.g., Rochester and Smylie, 1974).

In general, tidal deformations are small and yield periodic changes in the moments of inertia, such that $\dot{\mathcal{I}}\boldsymbol{\omega} \ll C\dot{\boldsymbol{\omega}}$ (e.g., Frouard and Efroimsky, 2018). Therefore, for simplicity, we can assume that the deformation is small with respect to the radius of the unperturbed sphere, R , such that $I_{ij} \ll C$ ($i, j = 1, 2, 3$), and

$$\mathbf{L} \approx C\boldsymbol{\omega} = C\boldsymbol{\omega} \mathbf{s} . \quad (4)$$

2.1 Potential energy of a non-spherical body

The gravitational potential of the central body at a generic position \mathbf{r} from its centre of mass is given by (e.g., Goldstein, 1950)

$$V(\mathbf{r}) = -\frac{\mathcal{G}m}{r} + \Delta V(\mathbf{r}) \quad (5)$$

with

$$\Delta V(\mathbf{r}) = \frac{3\mathcal{G}}{2r^3} \hat{\mathbf{r}} \cdot \mathcal{I} \cdot \hat{\mathbf{r}} , \quad (6)$$

where $r = \|\mathbf{r}\|$ is the norm, $\hat{\mathbf{r}} = \mathbf{r}/r = (\hat{x}_1, \hat{x}_2, \hat{x}_3)$ is the unit vector, and we neglect terms in $(R/r)^3$ (quadrupolar approximation).

The point mass m_0 interacts with the potential of the central body (Eq. (5)). The non-spherical contribution of this potential, $\Delta V(\mathbf{r})$, is responsible for the perturbations to the Keplerian motion. The corresponding potential energy, $U(\mathbf{r}) = m_0\Delta V(\mathbf{r})$, can be rewritten as

$$U(\mathbf{r}) = \frac{3\mathcal{G}m_0}{2r^3} \left[(I_{22} - I_{11})\left(\hat{x}_2^2 - \frac{1}{3}\right) + (I_{33} - I_{11})\left(\hat{x}_3^2 - \frac{1}{3}\right) + 2(I_{12}\hat{x}_1\hat{x}_2 + I_{13}\hat{x}_1\hat{x}_3 + I_{23}\hat{x}_2\hat{x}_3) \right] . \quad (7)$$

2.2 Reference frames

In this work we use two different reference frames, one attached to the orbit of the perturber and another to the spin axis of the central body (see Fig. 1). The reason for this choice is that the unit vectors \mathbf{k} and \mathbf{s} are easily directly obtained from the orbital (Eq. (1)) and rotational (Eq. (4)) angular momentum vectors, respectively. In general, these two vectors are not collinear, and so in a first step we need to build two independent frames as in Correia (2006).

We let $(\hat{\mathbf{e}}, \mathbf{k} \times \hat{\mathbf{e}}, \mathbf{k})$ to be a cartesian frame such that \mathbf{k} is aligned with the normal to the orbit, and $\hat{\mathbf{e}} = \mathbf{e}/e$ is aligned with the pericentre of the orbit and obtained from the Laplace vector

$$\mathbf{e} = \frac{\dot{\mathbf{r}} \times \mathbf{G}}{\beta\mu} - \hat{\mathbf{r}} . \quad (8)$$

We further let $(\mathbf{p}, \mathbf{q}, \mathbf{s})$ to be a cartesian frame, such that

$$\mathbf{p} = \frac{\mathbf{k} \times \mathbf{s}}{\sin\theta} , \quad \mathbf{q} = \mathbf{s} \times \mathbf{p} = \frac{\mathbf{k} - \cos\theta \mathbf{s}}{\sin\theta} , \quad (9)$$

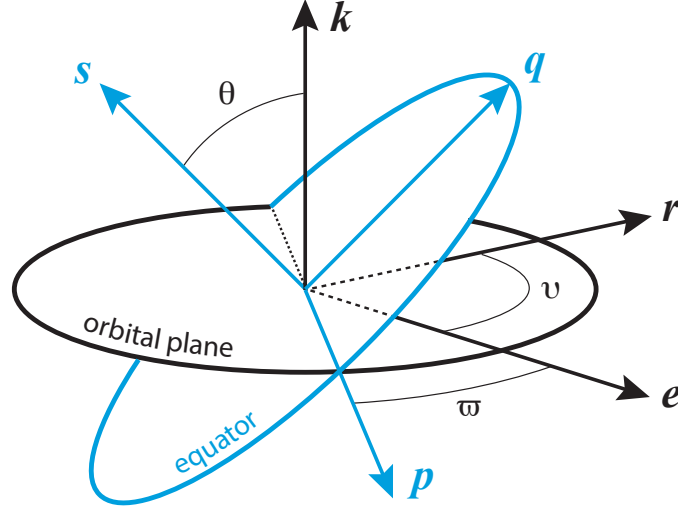


Fig. 1 Reference frames and angles. $(\hat{\mathbf{e}}, \mathbf{k} \times \hat{\mathbf{e}}, \mathbf{k})$ is a cartesian frame such that \mathbf{k} is a unit vector normal to the orbital plane, \mathbf{e} is the Laplace-Runge-Lenz vector (where $\hat{\mathbf{e}} = \mathbf{e}/e$ gives the direction of the pericentre), ϖ is the argument of the pericentre and v is the true anomaly. $(\mathbf{p}, \mathbf{q}, \mathbf{s})$ is a cartesian frame, such that \mathbf{s} is a unit vector normal to the equatorial plane of the central body, \mathbf{p} is a unit vector along the line of nodes of the two reference planes, and θ is the angle between them. Note that, although \mathbf{s} gives the direction of the spin axis, the vectors \mathbf{p} and $\mathbf{q} = \mathbf{s} \times \mathbf{p}$ follow the orbital plane and not the rotation.

where \mathbf{s} is aligned with the spin axis, and \mathbf{p} is aligned with the line of nodes between the equator of the central body and the orbital plane of the perturber (Fig. 1). The angle θ corresponds to the angle between \mathbf{k} and \mathbf{s} , that is, $\cos \theta = \mathbf{k} \cdot \mathbf{s}$.

These two frames are also known as “precession frames”, as they follow the precession of the pericentre and node, respectively. They are connected through the rotation matrix

$$\begin{bmatrix} \hat{\mathbf{e}} \\ \mathbf{k} \times \hat{\mathbf{e}} \\ \mathbf{k} \end{bmatrix} = \begin{bmatrix} \cos \varpi & \cos \theta \sin \varpi & -\sin \theta \sin \varpi \\ -\sin \varpi & \cos \theta \cos \varpi & -\sin \theta \cos \varpi \\ 0 & \sin \theta & \cos \theta \end{bmatrix} \begin{bmatrix} \mathbf{p} \\ \mathbf{q} \\ \mathbf{s} \end{bmatrix}, \quad (10)$$

where ϖ is the argument of the pericentre. We note that these two frames are not inertial, because the orbit and the spin can evolve due to tidal interactions. However, the changes are very small during an orbital period, and so the two frames can be assumed as constant.

The position vector can be expressed in these two frames as

$$\hat{\mathbf{r}} = \cos v \hat{\mathbf{e}} + \sin v \mathbf{k} \times \hat{\mathbf{e}} = \hat{x}_1 \mathbf{p} + \hat{x}_2 \mathbf{q} + \hat{x}_3 \mathbf{s}, \quad (11)$$

where v is the true anomaly, and

$$\begin{aligned} \hat{x}_1 &= \hat{\mathbf{r}} \cdot \mathbf{p} = \cos v \hat{\mathbf{e}} \cdot \mathbf{p} + \sin v \frac{\hat{\mathbf{e}} \cdot \mathbf{s}}{\sin \theta} = \cos(\varpi + v), \\ \hat{x}_2 &= \hat{\mathbf{r}} \cdot \mathbf{q} = -\cos v \frac{\cos \theta \hat{\mathbf{e}} \cdot \mathbf{s}}{\sin \theta} + \sin v \cos \theta \hat{\mathbf{e}} \cdot \mathbf{p} = \cos \theta \sin(\varpi + v), \\ \hat{x}_3 &= \hat{\mathbf{r}} \cdot \mathbf{s} = \cos v \hat{\mathbf{e}} \cdot \mathbf{s} - \sin v \sin \theta \hat{\mathbf{e}} \cdot \mathbf{p} = -\sin \theta \sin(\varpi + v). \end{aligned} \quad (12)$$

Similarly,

$$\dot{\mathbf{r}} = \frac{na}{\sqrt{1-e^2}} \mathbf{k} \times (\hat{\mathbf{r}} + \mathbf{e}) = \frac{na}{\sqrt{1-e^2}} ((\cos v + e) \mathbf{k} \times \hat{\mathbf{e}} - \sin v \hat{\mathbf{e}}) , \quad (13)$$

with

$$\begin{aligned} \dot{\mathbf{r}} \cdot \mathbf{p} &= \frac{-na}{\sqrt{1-e^2}} (\sin(\varpi + v) + e \sin \varpi) , \\ \dot{\mathbf{r}} \cdot \mathbf{q} &= \frac{na}{\sqrt{1-e^2}} \cos \theta (\cos(\varpi + v) + e \cos \varpi) , \\ \dot{\mathbf{r}} \cdot \mathbf{s} &= \frac{-na}{\sqrt{1-e^2}} \sin \theta (\cos(\varpi + v) + e \cos \varpi) , \end{aligned} \quad (14)$$

where $n = \sqrt{\mu/a^3}$ is the mean motion.

2.3 Equations of motion

The tidal force between the two bodies is easily obtained from the potential energy (Eq. (7)) as

$$\mathbf{F} = -\nabla U(\mathbf{r}) = \mathbf{F}_1 + \mathbf{F}_2 , \quad (15)$$

with

$$\mathbf{F}_1 = \frac{15\mathcal{G}m_0}{r^4} \left[\frac{I_{22} - I_{11}}{2} (\hat{x}_2^2 - \frac{1}{5}) + \frac{I_{33} - I_{11}}{2} (\hat{x}_3^2 - \frac{1}{5}) + I_{12}\hat{x}_1\hat{x}_2 + I_{13}\hat{x}_1\hat{x}_3 + I_{23}\hat{x}_2\hat{x}_3 \right] \hat{\mathbf{r}} , \quad (16)$$

and

$$\begin{aligned} \mathbf{F}_2 &= -\frac{3\mathcal{G}m_0}{r^4} \left[(I_{22} - I_{11})\hat{x}_2 \mathbf{q} + (I_{33} - I_{11})\hat{x}_3 \mathbf{s} \right. \\ &\quad \left. + I_{12}(\hat{x}_1 \mathbf{q} + \hat{x}_2 \mathbf{p}) + I_{13}(\hat{x}_1 \mathbf{s} + \hat{x}_3 \mathbf{p}) + I_{23}(\hat{x}_2 \mathbf{s} + \hat{x}_3 \mathbf{q}) \right] . \end{aligned} \quad (17)$$

We decompose \mathbf{F} and the following vectorial quantities in the frame $(\mathbf{p}, \mathbf{q}, \mathbf{s})$, as this greatly facilitates the computation of the inertia tensor \mathcal{I} (Sect. 2.5). There is no loss of generality with this choice, because the vectors $(\mathbf{p}, \mathbf{q}, \mathbf{s})$ can always be expressed in another basis. In particular, we follow the evolution of the system in an inertial frame, since nothing forbids to project an inertial vector on a non-inertial coordinate system. We obtain for the orbital evolution of the system

$$\ddot{\mathbf{r}} = -\frac{\mu}{r^2} \hat{\mathbf{r}} + \frac{\mathbf{F}}{\beta} . \quad (18)$$

The first term corresponds to the Keplerian motion, while the second one corresponds to the correction from the tidal force. From a secular evolution perspective, we only care about the modifications in the orbit and spin that are brought by the second term. Therefore, the evolution of the systems is better described by the evolution of \mathbf{G} and \mathbf{e} for the orbit and \mathbf{L} for the spin.

The evolution of the angular momentum vectors is computed from the gravitational torque. In an inertial frame, we have:

$$\dot{\mathbf{G}} = \mathbf{T} = \mathbf{r} \times \mathbf{F} = \mathbf{r} \times \mathbf{F}_2 , \quad (19)$$

and, owing to the conservation of the total angular momentum,

$$\dot{\mathbf{L}} = -\dot{\mathbf{G}} = -\mathbf{T} , \quad (20)$$

with

$$\begin{aligned} \mathbf{T} = & -\frac{3\mathcal{G}m_0}{r^3} \left\{ \left[(I_{33} - I_{22})\hat{x}_2\hat{x}_3 - I_{12}\hat{x}_1\hat{x}_3 + I_{13}\hat{x}_1\hat{x}_2 + I_{23}(\hat{x}_2^2 - \hat{x}_3^2) \right] \mathbf{p} \right. \\ & + \left[(I_{11} - I_{33})\hat{x}_1\hat{x}_3 + I_{12}\hat{x}_2\hat{x}_3 + I_{13}(\hat{x}_3^2 - \hat{x}_1^2) - I_{23}\hat{x}_1\hat{x}_2 \right] \mathbf{q} \\ & \left. + \left[(I_{22} - I_{11})\hat{x}_1\hat{x}_2 + I_{12}(\hat{x}_1^2 - \hat{x}_2^2) - I_{13}\hat{x}_2\hat{x}_3 + I_{23}\hat{x}_1\hat{x}_3 \right] \mathbf{s} \right\}. \end{aligned} \quad (21)$$

The evolution of the Laplace vector is obtained by differentiating expression (8)

$$\dot{\mathbf{e}} = \frac{1}{\beta\mu} \left(\frac{\mathbf{F}}{\beta} \times \mathbf{G} + \dot{\mathbf{r}} \times \mathbf{T} \right). \quad (22)$$

2.4 Deformation of the central body

The mass distribution inside the central body is characterised by the coefficients of the inertia tensor, \mathcal{I} (Eq. (3)). It is the result of self gravity and the response to any perturbing potential. Here, we consider that the central body is an extended body that deforms solely under the action of the differential gravitational force from the companion body of mass m_0 . A mass element dm at a location \mathbf{r}' is thus subject to the perturbing potential (e.g. [Lambeck, 1980](#))

$$V_p(\mathbf{r}') = -\frac{\mathcal{G}m_0}{r} \left(\frac{r'}{r} \right)^2 P_2(\hat{\mathbf{r}}' \cdot \hat{\mathbf{r}}), \quad (23)$$

where \mathbf{r} is the position of the mass m_0 with respect to the centre of mass of the central body, $P_2(x) = (3x^2 - 1)/2$ is a Legendre polynomial, and we neglected terms higher than $(r'/r)^3$, that is, we consider only the quadrupole perturbations. Thus, on the central body's surface, \mathbf{R} , the non-spherical contribution of the perturbing potential is given by

$$V_p(\mathbf{R}) = -\frac{\mathcal{G}m_0}{r} \left(\frac{R}{r} \right)^2 P_2(\hat{\mathbf{R}} \cdot \hat{\mathbf{r}}), \quad (24)$$

where $R = |\mathbf{R}|$. For simplicity, since the surface of the central body is nearly spherical, we can assume R to be constant and equal to the average radius.

The above potential can be rearranged as

$$V_p(\mathbf{R}) = \frac{3\mathcal{G}}{2R^3} \hat{\mathbf{R}} \cdot \mathcal{I}_p \cdot \hat{\mathbf{R}}, \quad (25)$$

with

$$\frac{\mathcal{I}_p}{mR^2} = -\frac{m_0}{m} \left(\frac{R}{r} \right)^3 \left(\hat{\mathbf{r}} \hat{\mathbf{r}}^T - \frac{1}{3} \mathbb{I} \right), \quad (26)$$

where T denotes the transpose, and \mathbb{I} is the identity matrix. The ‘‘perturbing’’ tensor \mathcal{I}_p can be seen as a perturbation of the inertia tensor, \mathcal{I} (Eq. (3)).

A convenient way of handling the deformation is through the Love number approach (e.g. [Love, 1927](#); [Peltier, 1974](#)). It assumes that the deformations are small and can be made linear, that is, proportional to the perturbing potential. The total tidal potential is thus a linear combination of the tidal responses to each excitation $V_p(\mathbf{R}, t')$ over time, with $t' \leq t$. In the frame of the central body, B , for any point of its surface we thus have

$$\Delta V(\mathbf{R}, t) = \int k_2(t - t') V_p(\mathbf{R}, t') dt' = k_2(t) * V_p(\mathbf{R}, t), \quad (27)$$

where $*$ is the convolution product. $k_2(t)$ is a *Love distribution* such that $k_2(t) = 0$ for all $t < 0$, which depends on the internal structure of the central body (for more details see Boué et al, 2016, 2019). The knowledge of $\Delta V(\mathbf{R}, t)$ is sufficient to constrain $\Delta V(\mathbf{r}, t)$, because it is the solution of a Dirichlet problem. Therefore, by comparing expressions (25) and (27) with the gravitational potential (Eq. (6)) taken at the central body's surface ($\mathbf{r} = \mathbf{R}$), we finally get for the deformation

$$\mathcal{I}^B(t) = \int k_2(t-t') \mathcal{I}_p^B(t') dt' = k_2(t) * \mathcal{I}_p^B(t) , \quad (28)$$

where \mathcal{I}^B and \mathcal{I}_p^B are the inertia (Eq. (3)) and the perturbing (Eq. (26)) tensors, respectively, expressed in the frame of the central body.

2.5 Deformation in the frequency domain

The inertia tensor in the frequency domain can be obtained by performing a Fourier transform

$$\hat{\mathcal{I}}^B(\sigma) = \int \mathcal{I}^B(t) e^{-i\sigma t} dt = \hat{k}_2(\sigma) \hat{\mathcal{I}}_p^B(\sigma) , \quad (29)$$

where

$$\hat{k}_2(\sigma) = \int k_2(t) e^{-i\sigma t} dt \quad (30)$$

is the second Love number, and we applied the properties of the convolution product. $\hat{k}_2(\sigma)$ is a complex number, whose modulus gives the amplitude of the tidal deformation and the argument gives the phase lag between the perturbation and the deformation. It follows that the deformation in the body frame (Eq. (28)) is much easier to compute in the frequency domain (Eq. (29)). However, it is a bit more difficult to compute the deformation in an arbitrary frame.

We let \mathcal{S} be the rotation matrix that allows us to convert any vector \mathbf{u}_B in a frame attached to the central body into another frame \mathbf{u} , such that $\mathbf{u} = \mathcal{S} \mathbf{u}_B$,

$$\mathcal{I}(t) = \mathcal{S}(t) \mathcal{I}^B(t) \mathcal{S}(t)^T , \quad \text{and} \quad \mathcal{I}_p(t) = \mathcal{S}(t) \mathcal{I}_p^B(t) \mathcal{S}(t)^T . \quad (31)$$

Then

$$\begin{aligned} \hat{\mathcal{I}}(\sigma) &= \int \mathcal{I}(t) e^{-i\sigma t} dt = \int \mathcal{S}(t) \mathcal{I}^B(t) \mathcal{S}(t)^T e^{-i\sigma t} dt \\ &= \int \int k_2(t-t') \mathcal{S}(t) \mathcal{I}_p^B(t') \mathcal{S}(t)^T e^{-i\sigma t} dt' dt \\ &= \int \int k_2(\tau) \mathcal{S}(t'+\tau) \mathcal{I}_p^B(t') \mathcal{S}(t'+\tau)^T e^{-i\sigma(t'+\tau)} dt' d\tau . \end{aligned} \quad (32)$$

Since $\mathcal{S}(t)$ is a rotation matrix, we note that $\mathcal{S}(t'+\tau) = \mathcal{S}(\tau) \mathcal{S}(t')$, thus

$$\begin{aligned} \hat{\mathcal{I}}(\sigma) &= \int \int k_2(\tau) \mathcal{S}(\tau) \mathcal{I}_p^B(t') \mathcal{S}(\tau)^T e^{-i\sigma(t'+\tau)} dt' d\tau \\ &= \int k_2(\tau) \mathcal{S}(\tau) \hat{\mathcal{I}}_p^B(\sigma) \mathcal{S}(\tau)^T e^{-i\sigma\tau} d\tau . \end{aligned} \quad (33)$$

At this stage, we need to explicit $\mathcal{S}(\tau)$ to proceed. For simplicity, we adopt the frame $(\mathbf{p}, \mathbf{q}, \mathbf{s})$, for which we have already obtained the equations of motion (Sect. 2.3), and where \mathbf{s} is the spin axis (Fig. 1). Since the central body rotates about the \mathbf{s} axis with velocity ω , we have

$$\mathcal{S}(\tau) = \begin{bmatrix} \cos \omega\tau & -\sin \omega\tau & 0 \\ \sin \omega\tau & \cos \omega\tau & 0 \\ 0 & 0 & 1 \end{bmatrix} , \quad (34)$$

which gives

$$\mathcal{S}(\tau) \hat{\mathcal{I}}_p(\sigma) \mathcal{S}(\tau)^T = \begin{bmatrix} -\Delta \hat{I}^p \cos 2\omega\tau - \hat{I}_{12}^p \sin 2\omega\tau - \frac{1}{2} \hat{I}_{33}^p, & -\Delta \hat{I}^p \sin 2\omega\tau + \hat{I}_{12}^p \cos 2\omega\tau, & \hat{I}_{13}^p \cos \omega\tau - \hat{I}_{23}^p \sin \omega\tau \\ -\Delta \hat{I}^p \sin 2\omega\tau + \hat{I}_{12}^p \cos 2\omega\tau, & \Delta \hat{I}^p \cos 2\omega\tau + \hat{I}_{12}^p \sin 2\omega\tau - \frac{1}{2} \hat{I}_{33}^p, & \hat{I}_{13}^p \sin \omega\tau + \hat{I}_{23}^p \cos \omega\tau \\ \hat{I}_{13}^p \cos \omega\tau - \hat{I}_{23}^p \sin \omega\tau, & \hat{I}_{13}^p \sin \omega\tau + \hat{I}_{23}^p \cos \omega\tau, & \hat{I}_{33}^p \end{bmatrix}, \quad (35)$$

where $\Delta \hat{I}^p = \frac{1}{2}(\hat{I}_{22}^p - \hat{I}_{11}^p)$. We thus have, for instance,

$$\begin{aligned} \hat{I}_{13}(\sigma) &= \int k_2(\tau) \left[\hat{I}_{13}^p(\sigma) \cos \omega\tau - \hat{I}_{23}^p(\sigma) \sin \omega\tau \right] e^{-i\sigma\tau} d\tau \\ &= \hat{I}_{13}^p(\sigma) \int k_2(\tau) \cos \omega\tau e^{-i\sigma\tau} d\tau - \hat{I}_{23}^p(\sigma) \int k_2(\tau) \sin \omega\tau e^{-i\sigma\tau} d\tau \\ &= \frac{1}{2} \hat{k}_2(\sigma - \omega) \left[\hat{I}_{13}^p(\sigma) + i \hat{I}_{23}^p(\sigma) \right] + \frac{1}{2} \hat{k}_2(\sigma + \omega) \left[\hat{I}_{13}^p(\sigma) - i \hat{I}_{23}^p(\sigma) \right]. \end{aligned} \quad (36)$$

Similarly, we obtain for the remaining coefficients of $\hat{\mathcal{I}}(\sigma)$:

$$\hat{I}_{23}(\sigma) = \frac{1}{2} \hat{k}_2(\sigma - \omega) \left[\hat{I}_{23}^p(\sigma) - i \hat{I}_{13}^p(\sigma) \right] + \frac{1}{2} \hat{k}_2(\sigma + \omega) \left[\hat{I}_{23}^p(\sigma) + i \hat{I}_{13}^p(\sigma) \right], \quad (37)$$

$$\hat{I}_{12}(\sigma) = \frac{1}{2} \hat{k}_2(\sigma - 2\omega) \left[\hat{I}_{12}^p(\sigma) + i \Delta \hat{I}^p(\sigma) \right] + \frac{1}{2} \hat{k}_2(\sigma + 2\omega) \left[\hat{I}_{12}^p(\sigma) - i \Delta \hat{I}^p(\sigma) \right], \quad (38)$$

$$\hat{I}_{33}(\sigma) = \hat{k}_2(\sigma) \hat{I}_{33}^p(\sigma), \quad (39)$$

$$\hat{I}_{22}(\sigma) = \Delta \hat{I}(\sigma) - \frac{1}{2} \hat{I}_{33}(\sigma), \quad (40)$$

$$\hat{I}_{11}(\sigma) = -\Delta \hat{I}(\sigma) - \frac{1}{2} \hat{I}_{33}(\sigma), \quad (41)$$

with

$$\Delta \hat{I}(\sigma) = \frac{1}{2} \hat{k}_2(\sigma - 2\omega) \left[\Delta \hat{I}^p(\sigma) - i \hat{I}_{12}^p(\sigma) \right] + \frac{1}{2} \hat{k}_2(\sigma + 2\omega) \left[\Delta \hat{I}^p(\sigma) + i \hat{I}_{12}^p(\sigma) \right]. \quad (42)$$

The coefficients of the inertia tensor \mathcal{I} (Eq. (3)) are now expressed in the frame $(\mathbf{p}, \mathbf{q}, \mathbf{s})$ and can be directly used in expressions (16), (17) and (21), provided that the coefficients of the perturbing tensor \mathcal{I}_p (Eq. (26)) are also given in this frame:

$$\frac{I_{11}^p}{mR^2} = -\frac{m_0}{m} \left(\frac{R}{r} \right)^3 \left(\hat{x}_1^2 - \frac{1}{3} \right), \quad \frac{I_{12}^p}{mR^2} = -\frac{m_0}{m} \left(\frac{R}{r} \right)^3 \hat{x}_1 \hat{x}_2, \quad (43)$$

$$\frac{I_{22}^p}{mR^2} = -\frac{m_0}{m} \left(\frac{R}{r} \right)^3 \left(\hat{x}_2^2 - \frac{1}{3} \right), \quad \frac{I_{23}^p}{mR^2} = -\frac{m_0}{m} \left(\frac{R}{r} \right)^3 \hat{x}_2 \hat{x}_3, \quad (44)$$

$$\frac{I_{33}^p}{mR^2} = -\frac{m_0}{m} \left(\frac{R}{r} \right)^3 \left(\hat{x}_3^2 - \frac{1}{3} \right), \quad \frac{I_{13}^p}{mR^2} = -\frac{m_0}{m} \left(\frac{R}{r} \right)^3 \hat{x}_1 \hat{x}_3. \quad (45)$$

2.6 Hansen coefficients

In order to use the coefficients of the inertia tensor $\hat{\mathcal{I}}(\sigma)$ (Eqs. (36)–(41)) in the equations of motion (Sect. 2.3) we need to return to the time domain using an inverse Fourier transform:

$$\mathcal{I}(t) = \int \hat{\mathcal{I}}(\sigma) e^{i\sigma t} d\sigma . \quad (46)$$

In general, the tidal perturbations introduced by the perturbing tensor $\mathcal{I}_p(t)$ are periodic and thus only a discrete number of frequencies exist, that is, we can express $\mathcal{I}(t)$ as a Fourier series:

$$\mathcal{I}(t) = \sum_k \hat{\mathcal{I}}(\sigma_k) e^{i\sigma_k t} . \quad (47)$$

In the frame $(\mathbf{p}, \mathbf{q}, \mathbf{s})$, the position of the perturber m_0 only depends on its orbital motion (Eq. (12)). Therefore, the only frequencies are the orbital mean motion, n , and its harmonics. A convenient way of expressing \mathcal{I}_p is through the Hansen coefficients, $X_k^{\ell, m}$ (e.g., Hughes, 1981):

$$\left(\frac{r}{a}\right)^\ell e^{imv} = \sum_{k=-\infty}^{+\infty} X_k^{\ell, m}(e) e^{ikM} , \quad (48)$$

with

$$X_k^{\ell, m}(e) = \frac{1}{2\pi} \int_{-\pi}^{\pi} \left(\frac{r}{a}\right)^\ell e^{i(mv - kM)} dM = \frac{1}{\pi} \int_0^\pi \left(\frac{1 - e^2}{1 + e \cos v}\right)^\ell \cos(mv - kM) dM . \quad (49)$$

For instance, for the I_{23}^p coefficient (Eq. (44)), we get from expression (12)

$$\begin{aligned} \frac{I_{23}^p}{mR^2} &= \frac{m_0}{m} \left(\frac{R}{r}\right)^3 \sin \theta \cos \theta \sin^2(\varpi + v) \\ &= \frac{1}{4} \frac{m_0}{m} \left(\frac{R}{a}\right)^3 \sin \theta \cos \theta \left(\frac{a}{r}\right)^3 \left(2 - e^{i2(\varpi+v)} - e^{-i2(\varpi+v)}\right) \\ &= \frac{1}{4} \frac{m_0}{m} \left(\frac{R}{a}\right)^3 \sin \theta \sum_{k=-\infty}^{+\infty} x \left(2X_k^{-3,0} - e^{i2\varpi} X_k^{-3,2} - e^{-i2\varpi} X_k^{-3,-2}\right) e^{ikM} , \end{aligned} \quad (50)$$

where $x = \cos \theta = \mathbf{k} \cdot \mathbf{s}$, and (Eq. (10))

$$e^{i\varpi} = \hat{\mathbf{e}} \cdot \mathbf{p} - i \frac{\hat{\mathbf{e}} \cdot \mathbf{s}}{\sin \theta} \quad \Rightarrow \quad e^{i2\varpi} = (\hat{\mathbf{e}} \cdot \mathbf{p})^2 - \left(\frac{\hat{\mathbf{e}} \cdot \mathbf{s}}{\sin \theta}\right)^2 - 2i (\hat{\mathbf{e}} \cdot \mathbf{p}) \left(\frac{\hat{\mathbf{e}} \cdot \mathbf{s}}{\sin \theta}\right) . \quad (51)$$

Similarly, for the I_{13}^p coefficient (Eq. (45)), we get

$$\frac{I_{13}^p}{mR^2} = \frac{1}{4i} \frac{m_0}{m} \left(\frac{R}{a}\right)^3 \sin \theta \sum_{k=-\infty}^{+\infty} \left(e^{i2\varpi} X_k^{-3,2} - e^{-i2\varpi} X_k^{-3,-2}\right) e^{ikM} . \quad (52)$$

Then, for the I_{23} coefficient we finally have (Eqs. (37) and (47))

$$\begin{aligned} I_{23} &= \frac{m_0 R^5}{8a^3} \sin \theta \sum_{k=-\infty}^{+\infty} \left[\hat{k}_2(kn - \omega) \left(2x X_k^{-3,0} - (1+x)e^{i2\varpi} X_k^{-3,2} + (1-x)e^{-i2\varpi} X_k^{-3,-2}\right) \right. \\ &\quad \left. + \hat{k}_2(kn + \omega) \left(2x X_k^{-3,0} + (1-x)e^{i2\varpi} X_k^{-3,2} - (1+x)e^{-i2\varpi} X_k^{-3,-2}\right) \right] e^{ikM} . \end{aligned} \quad (53)$$

k	$X_k^{-3,0}(e)$	$X_k^{-3,1}(e)$	$X_k^{-3,2}(e)$
-6	$\frac{3167}{320}e^6$	—	—
-5	$\frac{1773}{256}e^5$	$\frac{16289}{9216}e^6$	—
-4	$\frac{77}{16}e^4 + \frac{129}{160}e^6$	$\frac{643}{480}e^5$	$\frac{4}{45}e^6$
-3	$\frac{53}{16}e^3 + \frac{393}{256}e^5$	$\frac{131}{128}e^4 + \frac{237}{256}e^6$	$\frac{81}{1280}e^5$
-2	$\frac{9}{4}e^2 + \frac{7}{4}e^4 + \frac{141}{64}e^6$	$\frac{19}{24}e^3 + \frac{43}{48}e^5$	$\frac{1}{24}e^4 + \frac{7}{240}e^6$
-1	$\frac{3}{2}e + \frac{27}{16}e^3 + \frac{261}{128}e^5$	$\frac{5}{8}e^2 + \frac{5}{6}e^4 + \frac{3103}{3072}e^6$	$\frac{1}{48}e^3 + \frac{11}{768}e^5$
0	$1 + \frac{3}{2}e^2 + \frac{15}{8}e^4 + \frac{35}{16}e^6$	$\frac{1}{2}e + \frac{3}{4}e^3 + \frac{15}{16}e^5$	—
1	$\frac{3}{2}e + \frac{27}{16}e^3 + \frac{261}{128}e^5$	$1 + \frac{1}{2}e^2 + \frac{55}{64}e^4 + \frac{1177}{1152}e^6$	$-\frac{1}{2}e + \frac{1}{16}e^3 - \frac{5}{384}e^5$
2	$\frac{9}{4}e^2 + \frac{7}{4}e^4 + \frac{141}{64}e^6$	$\frac{5}{2}e - \frac{1}{8}e^3 + \frac{103}{96}e^5$	$1 - \frac{5}{2}e^2 + \frac{13}{16}e^4 - \frac{35}{288}e^6$
3	$\frac{53}{16}e^3 + \frac{393}{256}e^5$	$\frac{39}{8}e^2 - 2e^4 + \frac{1803}{1024}e^6$	$\frac{7}{2}e - \frac{123}{16}e^3 + \frac{489}{128}e^5$
4	$\frac{77}{16}e^4 + \frac{129}{160}e^6$	$\frac{103}{12}e^3 - \frac{593}{96}e^5$	$\frac{17}{2}e^2 - \frac{115}{6}e^4 + \frac{601}{48}e^6$
5	$\frac{1773}{256}e^5$	$\frac{5485}{384}e^4 - \frac{11053}{768}e^6$	$\frac{845}{48}e^3 - \frac{32525}{768}e^5$
6	$\frac{3167}{320}e^6$	$\frac{3669}{160}e^5$	$\frac{533}{16}e^4 - \frac{13827}{160}e^6$
7	—	$\frac{330911}{9216}e^6$	$\frac{228347}{3840}e^5$
8	—	—	$\frac{73369}{720}e^6$

Table 1 Hansen coefficients up to e^6 . The exact expression of these coefficients is given by expression (49).

Since the coefficients of the \mathcal{I}_p tensor are all $I_{ij}^p \propto r^{-3}$ (Eqs. (43)–(45)), in the expression of the inertia tensor \mathcal{I} can only appear Hansen coefficients of the kind $X_k^{-3,m}$. The same occurs with the torque (Eq. (21)). The force (Eq. (15)) and the derivative of the Laplace vector (Eq. (22)) are proportional to r^{-4} and we thus expect terms in $X_k^{-4,m}$. However, it is possible to provide the entire set of equations of motion only in terms of the coefficients $X_k^{-3,0}$, $X_k^{-3,1}$, and $X_k^{-3,2}$ (Table 1), by using some recurrence properties of the Hansen coefficients (see appendix A).

2.7 Tidal models

The tidal deformation of the central body is completely described by expression (47), where $\hat{\mathcal{I}}(\sigma)$ is obtained from the Love number $k_2(\sigma)$ combined with the perturbing tensor $\hat{\mathcal{I}}_p(\sigma)$ (Eqs. (36)–(41)). While the perturbing tensor is well determined, as it depends only on the position of the perturbing body (Eqs. (43)–(45)), the Love number is subject to large uncertainties, as it depends on the internal structure of the central body. Therefore, in order to compute $\hat{k}_2(\sigma)$ one needs to adopt some rheological model for the deformation. A large variety of models exist, but the most commonly used are the constant- Q (e.g., Munk and MacDonald, 1960), the linear model (e.g., Mignard, 1979), the Maxwell model (e.g., Correia et al, 2014), and the Andrade model (e.g., Efroimsky, 2012). Some models appear to be better suited to certain situations, but there is no model that is globally accepted. However, viscoelastic rheologies are usually more realistic as they are able to reproduce the main features of tidal dissipation (e.g. Remus et al, 2012). For a review of the main viscoelastic models see Renaud and Henning (2018). The Love number is a complex number, and so it can be decomposed in its real and imaginary parts as

$$\hat{k}_2(\sigma) = a(\sigma) - ib(\sigma) . \quad (54)$$

This partition is very useful when we write the equations of motion (see Sects. 3 and 4), because the imaginary part characterises the material's viscous phase lag and is thus directly related to the

amount of energy dissipated by tides. This is why we write expression (54) with a minus for the imaginary part, the deformation lags behind the perturbation and therefore the imaginary part is always negative. In addition, from expression (30) we have $\hat{k}_2^*(\sigma) = \hat{k}_2(-\sigma)$, and so $a(\sigma) = a(-\sigma)$ is always an even function and $b(\sigma) = -b(-\sigma)$ is always an odd function. Here, we provide the expressions of $a(\sigma)$ and $b(\sigma)$ for the more frequently used tidal models.

2.7.1 Constant- Q model

A commonly used dimensionless measure of the tidal dissipation is the quality factor

$$Q^{-1} = \frac{1}{2\pi E_0} \oint \dot{E} dt, \quad (55)$$

where the line integral over \dot{E} is the energy dissipated during one period of tidal stress, and E_0 is the peak energy stored in the system during the same period. In general, Q is a function of the frequency, and can be related to the Love number through (e.g., [Henning et al, 2009](#))

$$b(\sigma) = \frac{|\hat{k}_2(\sigma)|}{Q(\sigma)}. \quad (56)$$

The constant- Q model assumes that both the quality factor and the norm of the Love number are constant for all frequencies, that is, $Q(\sigma) = Q(0) = Q_0$ and $|\hat{k}_2(\sigma)| = |\hat{k}_2(0)| = k_f$. The quantity k_f is the fluid Love number, which corresponds to the maximal deformation resulting from a permanent perturbation and depends only on the internal structure of the central body. For instance, for a homogenous sphere, we have $k_f = 3/2$. Since $b(\sigma)$ is an odd function we have

$$a(\sigma) = k_f, \quad \text{and} \quad b(\sigma) = \frac{k_f}{Q_0} \text{sign}(\sigma). \quad (57)$$

The constant- Q model is appropriate for short evolution timescales, where the orbital and the spin frequencies do not change dramatically.

2.7.2 Linear or weak friction model

The linear or weak friction model assumes that the time delay, Δt , between the maximal deformation and the perturbation is constant and small ([Singer, 1968](#); [Alexander, 1973](#); [Mignard, 1979](#)). This is equivalent to assume that the Love distribution is a Dirac distribution (see [Boué et al, 2019](#))

$$k_2(t) = k_f \delta(t - \Delta t). \quad (58)$$

As a result, we have (Eq. (30))

$$\hat{k}_2(\sigma) = k_f e^{-i\sigma\Delta t} \approx k_f (1 - i\sigma\Delta t), \quad (59)$$

that is

$$a(\sigma) = k_f, \quad \text{and} \quad b(\sigma) = k_f \sigma \Delta t. \quad (60)$$

The time delay can be related to the Newton fluid relaxation time, $\Delta t = \tau_v$, with

$$\tau_v = \frac{38\pi\eta R^4}{3\mathcal{G}m^2}, \quad (61)$$

where η is the viscosity of the fluid. The linear model is appropriate for bodies with small viscosities. It is also a good approximation of other tidal models when $\sigma \approx 0$.

2.7.3 Maxwell model

A material is called a Maxwell solid when it responds to stresses like a massless, damped harmonic oscillator. It is characterised by a rigidity μ (or shear modulus), and by a viscosity η . It is one of the simplest viscoelastic models, where the material behaves like an elastic solid over short time scales ($\eta \rightarrow \infty$), but flows like a fluid over long periods of time ($\mu \rightarrow \infty$). The Love number for the Maxwell model is given by (e.g. [Darwin, 1908](#)):

$$\hat{k}_2(\sigma) = k_f \frac{1 + i\sigma\tau_e}{1 + i\sigma\tau}, \quad (62)$$

where $\tau_e = \eta/\mu$ is the elastic or Maxwell relaxation time and $\tau = \tau_e + \tau_v$. We thus have

$$a(\sigma) = k_f \frac{1 + \sigma^2\tau_e\tau}{1 + (\sigma\tau)^2}, \quad \text{and} \quad b(\sigma) = k_f \frac{\sigma\tau_v}{1 + (\sigma\tau)^2}. \quad (63)$$

The Maxwell model is appropriate for bodies with a rocky nature. For small tidal frequencies ($\sigma\tau \ll 1$) it is similar to the linear model, but for high tidal frequencies ($\sigma\tau \gg 1$) it becomes inversely proportional to the tidal frequency, σ . This feature gives rise to the appearance of non-synchronous spin-orbit resonances in this regime (e.g., [Correia et al, 2014](#)).

2.7.4 Andrade model

The Andrade model is also a viscoelastic model, but more complex than the Maxwell one. It is derived from laboratory measurements on the response of materials to stress. It can be represented by three mechanical elements combined in series, a spring, a dashpot and a spring-pot (e.g., [Andrade, 1910](#); [Ben Jazia et al, 2014](#); [Gevorgyan et al, 2020](#)). The Love number for the Andrade model is given by (e.g., [Efroimsky, 2012](#)):

$$\hat{k}_2(\sigma) = \frac{k_f}{1 + \hat{\mu}(\sigma)}, \quad (64)$$

where

$$\hat{\mu}(\sigma) = \frac{\tau_v}{\tau_e} \left[1 - i(\sigma\tau_e)^{-1} + (i\sigma\tau_a)^{-\alpha} \Gamma(1 + \alpha) \right]^{-1}, \quad (65)$$

is the effective rigidity. The parameter α is an empirical adjustable parameter whose value depends on the material, we usually have $0.2 \leq \alpha \leq 0.4$. The quantity τ_a is the timescale associated with the Andrade creep and may be termed as the ‘‘Andrade’’ or the ‘‘anelastic’’ time. Then,

$$a(\sigma) = k_f \left[1 - \frac{\mathcal{A}(\sigma) \sigma\tau_v}{\mathcal{A}(\sigma)^2 + \mathcal{B}(\sigma)^2} \right], \quad \text{and} \quad b(\sigma) = k_f \frac{\mathcal{B}(\sigma) \sigma\tau_v}{\mathcal{A}(\sigma)^2 + \mathcal{B}(\sigma)^2}, \quad (66)$$

with

$$\mathcal{A}(\sigma) = (\sigma\tau) \left[1 + |\sigma\tau|^{-\alpha} \left(\frac{\tau_e}{\tau} \right) \left(\frac{\tau}{\tau_a} \right)^\alpha \cos \left(\frac{\alpha\pi}{2} \right) \Gamma(1 + \alpha) \right], \quad (67)$$

and

$$\mathcal{B}(\sigma) = 1 + |\sigma\tau|^{1-\alpha} \left(\frac{\tau_e}{\tau} \right) \left(\frac{\tau}{\tau_a} \right)^\alpha \sin \left(\frac{\alpha\pi}{2} \right) \Gamma(1 + \alpha). \quad (68)$$

The Andrade model is also appropriate for bodies with a rocky nature, which includes the effect of transient creep response. As a result, for high tidal frequencies ($\sigma\tau \gg 1$) it dissipates more energy than in the case of the Maxwell model (see discussions in [Renaud and Henning, 2018](#)).

3 Average over the mean anomaly

In general, tidal effects slowly modify the spin and the orbit of the central body, in a timescale much longer than the orbital period of the system. Therefore, we can average the equations of motion (Sect. 2.3) over the mean anomaly and obtain the equations for the secular evolution of the system due to tidal effects.

In order to proceed with this calculation, we first need to expand the tidal torque (Eq. (21)) and the derivative of the Laplace vector (Eq. (22)) in Hansen coefficients (Eq. (48)). For instance, for the last term in the \mathbf{s} component of the tidal torque we have (Eq. (12))

$$\begin{aligned} -\frac{3\mathcal{G}m_0}{r^3} I_{23} \hat{x}_1 \hat{x}_3 &= \frac{3\mathcal{G}m_0}{2r^3} I_{23} \sin \theta \sin(2\varpi + 2\nu) \\ &= \frac{3\mathcal{G}m_0}{4ia^3} I_{23} \sin \theta \sum_{k'=-\infty}^{+\infty} \left(e^{i2\varpi} X_{k'}^{-3,2} - e^{-i2\varpi} X_{k'}^{-3,-2} \right) e^{ik'M}. \end{aligned} \quad (69)$$

Then, we replace the expression of I_{23} also expanded in Hansen coefficients (Eq. (53)), and average over the mean anomaly, M , which is equivalent to retain only the terms with $k' = -k$:

$$\begin{aligned} \left\langle -\frac{3\mathcal{G}m_0}{r^3} I_{23} \hat{x}_1 \hat{x}_3 \right\rangle_M &= \frac{3\mathcal{G}m_0^2 R^5}{32ia^6} \sin^2 \theta \sum_{k=-\infty}^{+\infty} \left(e^{i2\varpi} X_{-k}^{-3,2} - e^{-i2\varpi} X_{-k}^{-3,-2} \right) \times \\ &\quad \left[\hat{k}_2(kn - \omega) \left(2x X_k^{-3,0} - (1+x) e^{i2\varpi} X_k^{-3,2} + (1-x) e^{-i2\varpi} X_k^{-3,-2} \right) \right. \\ &\quad \left. + \hat{k}_2(kn + \omega) \left(2x X_k^{-3,0} + (1-x) e^{i2\varpi} X_k^{-3,2} - (1+x) e^{-i2\varpi} X_k^{-3,-2} \right) \right]. \end{aligned} \quad (70)$$

Finally, we decompose the Love number in its real and imaginary parts (Eq. (54)), make use of their parity properties, and use the simplification $X_{-k}^{-3,m} = X_k^{-3,-m}$ (Eq. (154)) to write

$$\begin{aligned} \left\langle -\frac{3\mathcal{G}m_0}{r^3} I_{23} \hat{x}_1 \hat{x}_3 \right\rangle_M &= \frac{3\mathcal{G}m_0^2 R^5}{16a^6} \sin^2 \theta \sum_{k=-\infty}^{+\infty} \left\{ b(\omega - kn) \left[2x \cos 2\varpi X_k^{-3,0} \left(X_k^{-3,-2} - X_k^{-3,2} \right) \right. \right. \\ &\quad \left. \left. - 2 \cos 4\varpi X_k^{-3,-2} X_k^{-3,2} + (1-x) \left(X_k^{-3,-2} \right)^2 + (1+x) \left(X_k^{-3,2} \right)^2 \right] \right. \\ &\quad \left. + 2x a(\omega - kn) \left[\sin 2\varpi X_k^{-3,0} \left(X_k^{-3,-2} + X_k^{-3,2} \right) - \sin 4\varpi X_k^{-3,-2} X_k^{-3,2} \right] \right\}, \end{aligned} \quad (71)$$

This last arrangement of the Love number is very useful, because terms in $a(\sigma)$ correspond to conservative contributions to the equations of motion, while the terms in $b(\sigma)$ are responsible for the dissipation and consequent tidal evolution. In addition, we are able to combine terms in $\hat{k}_2(\omega \pm kn)$ in a single term $\hat{k}_2(\omega - kn)$.

3.1 Tidal torque

The tidal torque is responsible for the variations that occur in the angular momenta (Eqs. (19) and (20)). In the reference frame $(\mathbf{p}, \mathbf{q}, \mathbf{s})$ its average value is obtained from expression (21) as

$$\langle \mathbf{T} \rangle_M = T_p \mathbf{p} + T_q \mathbf{q} + T_s \mathbf{s}. \quad (72)$$

However, we verify there exist some interesting symmetries in the expression of the average torque, which simplifies if we introduce two additional projections

$$\langle \mathbf{T} \rangle_M = \hat{T}_p \mathbf{p} + \hat{T}_q \mathbf{q} + \hat{T}_s \mathbf{s} + T_4 \hat{\mathbf{e}} + T_5 \mathbf{s} \times \hat{\mathbf{e}}, \quad (73)$$

with

$$\hat{T}_p = T_p - T_4 \hat{\mathbf{e}} \cdot \mathbf{p} + T_5 \hat{\mathbf{e}} \cdot \mathbf{q}, \quad \hat{T}_q = T_q - T_5 \hat{\mathbf{e}} \cdot \mathbf{p} - T_4 \hat{\mathbf{e}} \cdot \mathbf{q}, \quad \hat{T}_s = T_s - T_4 \hat{\mathbf{e}} \cdot \mathbf{s}, \quad (74)$$

or,

$$\hat{T}_p = T_p + \frac{T_4 z - T_5 xy}{\sin \theta}, \quad \hat{T}_q = T_q + \frac{T_4 xy + T_5 z}{\sin \theta}, \quad \hat{T}_s = T_s - T_4 y, \quad (75)$$

where we used the following notations:

$$x = \mathbf{k} \cdot \mathbf{s} = \cos \theta, \quad y = \hat{\mathbf{e}} \cdot \mathbf{s} = -\sin \theta \sin \varpi, \quad \text{and} \quad z = (\mathbf{k} \times \hat{\mathbf{e}}) \cdot \mathbf{s} = -\sin \theta \cos \varpi. \quad (76)$$

This rearrangement of the projections removes apparent singularities for $e = 0$, since all terms in $\cos \varpi$ and $\sin \varpi$ are transferred to the Laplace vector \mathbf{e} (Eq. (51)). Similarly, in order to remove the apparent singularities for $\theta = 0$ we finally write

$$\langle \mathbf{T} \rangle_M = T_1 \mathbf{k} + T_2 \mathbf{s} + T_3 \mathbf{k} \times \mathbf{s} + T_4 \hat{\mathbf{e}} + T_5 \mathbf{s} \times \hat{\mathbf{e}}, \quad (77)$$

with

$$T_1 = \frac{\hat{T}_q}{\sin \theta}, \quad T_2 = \left(\hat{T}_s - \cos \theta \frac{\hat{T}_q}{\sin \theta} \right), \quad T_3 = \frac{\hat{T}_p}{\sin \theta}. \quad (78)$$

The expressions of the coefficients T_1, \dots, T_5 do not present any singularities and can be obtained solely from the angular momentum and Laplace unit vectors as

$$\begin{aligned} T_1 = -\mathcal{T}_0 \sum_{k=-\infty}^{+\infty} & \left\{ \frac{3}{32} b(-kn) \left[3(1-x^2) \left((X_k^{-3,-2})^2 - (X_k^{-3,2})^2 \right) \right. \right. \\ & \left. \left. - 2(1-3x^2-2y^2) X_k^{-3,0} (X_k^{-3,-2} - X_k^{-3,2}) \right] \right. \\ & + \frac{3}{16} b(\omega - kn) \left[4x^3 (X_k^{-3,0})^2 + (1-x)^2 (2+x) (X_k^{-3,-2})^2 - (1+x)^2 (2-x) (X_k^{-3,2})^2 \right. \\ & \left. + 4x(1-x^2-y^2) X_k^{-3,0} (X_k^{-3,-2} + X_k^{-3,2}) - 2x(1-x^2-4y^2) X_k^{-3,2} X_k^{-3,-2} \right] \\ & + \frac{3}{16} b(2\omega - kn) \left[2x(1-x^2) (X_k^{-3,0})^2 + \frac{1}{2} (1-x)^3 (X_k^{-3,-2})^2 - \frac{1}{2} (1+x)^3 (X_k^{-3,2})^2 \right. \\ & \left. + \left((1-x)^2 (1+2x) - 2(1-x)y^2 \right) X_k^{-3,0} X_k^{-3,-2} - \left((1+x)^2 (1-2x) - 2(1+x)y^2 \right) X_k^{-3,0} X_k^{-3,2} \right. \\ & \left. \left. + x(1-x^2-4y^2) X_k^{-3,2} X_k^{-3,-2} \right] \right\}, \quad (79) \end{aligned}$$

$$\begin{aligned}
T_2 = \mathcal{T}_0 \sum_{k=-\infty}^{+\infty} & \left\{ \frac{3}{32} b(-kn) x \left[3(1-x^2) \left((X_k^{-3,-2})^2 - (X_k^{-3,2})^2 \right) \right. \right. \\
& - 2(1-3x^2-6y^2) X_k^{-3,0} (X_k^{-3,-2} - X_k^{-3,2}) \left. \right] \\
& + \frac{3}{16} b(\omega - kn) \left[4x^2 (X_k^{-3,0})^2 + (1-x)^2 (1+2x) (X_k^{-3,-2})^2 + (1+x)^2 (1-2x) (X_k^{-3,2})^2 \right. \\
& + 4y^2 X_k^{-3,0} (X_k^{-3,-2} + X_k^{-3,2}) + 4x(1-x^2-2y^2) X_k^{-3,0} (X_k^{-3,-2} - X_k^{-3,2}) \\
& \left. - 2(1-x^2-4y^2) X_k^{-3,2} X_k^{-3,-2} \right] \\
& + \frac{3}{32} b(2\omega - kn) \left[4(1-x^2) (X_k^{-3,0})^2 + (1-x)^3 (X_k^{-3,-2})^2 + (1+x)^3 (X_k^{-3,2})^2 \right. \\
& + 4(1-y^2) X_k^{-3,0} (X_k^{-3,-2} + X_k^{-3,2}) - 2x(3-x^2-2y^2) X_k^{-3,0} (X_k^{-3,-2} - X_k^{-3,2}) \\
& \left. + 2(1-x^2-4y^2) X_k^{-3,2} X_k^{-3,-2} \right] \left. \right\}, \tag{80}
\end{aligned}$$

$$\begin{aligned}
T_3 = -\mathcal{T}_0 \sum_{k=-\infty}^{+\infty} & \left\{ \frac{3}{16} x a(-kn) \left[2(1-3x^2) (X_k^{-3,0})^2 + \frac{3}{2} (1-x^2) \left((X_k^{-3,-2})^2 + (X_k^{-3,2})^2 \right) \right. \right. \\
& - 2(2-3(x^2+y^2)) X_k^{-3,0} (X_k^{-3,-2} + X_k^{-3,2}) + 3(1-x^2-4y^2) X_k^{-3,2} X_k^{-3,-2} \left. \right] \\
& - \frac{3}{16} a(\omega - kn) \left[4x(1-2x^2) (X_k^{-3,0})^2 - (1-x)^2 (1+2x) (X_k^{-3,-2})^2 + (1+x)^2 (1-2x) (X_k^{-3,2})^2 \right. \\
& + 2((1-x)(1-x-4x^2) - 2(1-2x)y^2) X_k^{-3,0} X_k^{-3,-2} \\
& \left. - 2((1+x)(1+x-4x^2) - 2(1+2x)y^2) X_k^{-3,0} X_k^{-3,2} + 4x(1-x^2-4y^2) X_k^{-3,2} X_k^{-3,-2} \right] \\
& + \frac{3}{16} a(2\omega - kn) \left[2x(1-x^2) (X_k^{-3,0})^2 + \frac{1}{2} (1-x)^3 (X_k^{-3,-2})^2 - \frac{1}{2} (1+x)^3 (X_k^{-3,2})^2 \right. \\
& + \left((1-x)^2 (1+2x) - 2(1-x)y^2 \right) X_k^{-3,0} X_k^{-3,-2} - \left((1+x)^2 (1-2x) - 2(1+x)y^2 \right) X_k^{-3,0} X_k^{-3,2} \\
& \left. + x(1-x^2-4y^2) X_k^{-3,2} X_k^{-3,-2} \right] \left. \right\}, \tag{81}
\end{aligned}$$

$$\begin{aligned}
T_4 = -\mathcal{T}_0 \sum_{k=-\infty}^{+\infty} & \left\{ \frac{3}{4} b(-kn) xy X_k^{-3,0} (X_k^{-3,-2} - X_k^{-3,2}) \right. \\
& + \frac{3}{4} y b(\omega - kn) \left[(1-x^2) X_k^{-3,0} (X_k^{-3,-2} + X_k^{-3,2}) - 2(1-x^2-2y^2) X_k^{-3,2} X_k^{-3,-2} \right] \\
& \left. + \frac{3}{8} y b(2\omega - kn) \left[(1-x)^2 X_k^{-3,0} X_k^{-3,-2} + (1+x)^2 X_k^{-3,0} X_k^{-3,2} + 2(1-x^2-2y^2) X_k^{-3,2} X_k^{-3,-2} \right] \right\}, \tag{82}
\end{aligned}$$

$$\begin{aligned}
T_5 = -\mathcal{T}_0 \sum_{k=-\infty}^{+\infty} & \left\{ \frac{3}{8} y a(-kn) \left[(1-3x^2) X_k^{-3,0} (X_k^{-3,-2} + X_k^{-3,2}) - 6(1-x^2-2y^2) X_k^{-3,2} X_k^{-3,-2} \right] \right. \\
& - \frac{3}{2} y a(\omega - kn) \left[x(1-x) X_k^{-3,0} X_k^{-3,-2} - x(1+x) X_k^{-3,0} X_k^{-3,2} - 2(1-x^2-2y^2) X_k^{-3,2} X_k^{-3,-2} \right] \\
& \left. - \frac{3}{8} y a(2\omega - kn) \left[(1-x)^2 X_k^{-3,0} X_k^{-3,-2} + (1+x)^2 X_k^{-3,0} X_k^{-3,2} + 2(1-x^2-2y^2) X_k^{-3,2} X_k^{-3,-2} \right] \right\}, \tag{83}
\end{aligned}$$

where

$$\mathcal{T}_0 = \frac{\mathcal{G}m_0^2 R^5}{a^6}. \tag{84}$$

We note that terms in $y = \hat{\mathbf{e}} \cdot \mathbf{s}$ only appear combined with the product of two different Hansen coefficients. This product is proportional to e^2 (Table 1) and therefore there is no problem if we are unable to accurately obtain $\hat{\mathbf{e}}$ from \mathbf{e} to compute y when $e \approx 0$. We also note that the coefficients T_1 , T_2 , and T_4 solely depend on $b(\sigma)$, thus contributing to a secular evolution of the angular momenta, while the coefficients T_3 and T_5 solely depend on $a(\sigma)$, thus resulting only in a precession of the angular momentum vectors.

3.2 Laplace vector

The Laplace vector is responsible for the variations that occur in the eccentricity and argument of the pericentre (Eq. (22)). As for the torque (Eq. (72)), we first need to express $\dot{\mathbf{e}}$ in the reference frame $(\mathbf{p}, \mathbf{q}, \mathbf{s})$, such that we can write the expression of \mathcal{I} using Love numbers and the Hansen coefficients (Eq. (53)). However, since the Laplace vector is attached to the orbital plane (Fig. 1), its expression becomes simpler if we project it on the frame $(\hat{\mathbf{e}}, \mathbf{k} \times \hat{\mathbf{e}}, \mathbf{k})$, which can be done by inverting expression (10). Moreover, two of the projections in this new frame directly give the variation of the eccentricity and the argument of the pericentre. Therefore, after averaging over the mean anomaly and rewriting the Hansen coefficients in the format $X_k^{-3,m}$ (appendix A), we get

$$\langle \dot{\mathbf{e}} \rangle_M = \dot{e} \hat{\mathbf{e}} + \dot{\phi} \mathbf{k} + e \dot{\omega} \mathbf{k} \times \hat{\mathbf{e}}, \quad (85)$$

with

$$\begin{aligned} \dot{e} = & -\mathcal{E}_0 \frac{\sqrt{1-e^2}}{e} \sum_{k=-\infty}^{+\infty} \left\{ \frac{3}{8} yz a(-kn) \left[(1-3x^2) X_k^{-3,0} (X_k^{-3,-2} + X_k^{-3,2}) - 6(1-x^2-2y^2) X_k^{-3,2} X_k^{-3,-2} \right] \right. \\ & - \frac{3}{2} yz a(\omega - kn) \left[x(1-x) X_k^{-3,0} X_k^{-3,-2} - x(1+x) X_k^{-3,0} X_k^{-3,2} - 2(1-x^2-2y^2) X_k^{-3,2} X_k^{-3,-2} \right] \\ & - \frac{3}{8} yz a(2\omega - kn) \left[(1-x)^2 X_k^{-3,0} X_k^{-3,-2} + (1+x)^2 X_k^{-3,0} X_k^{-3,2} + 2(1-x^2-2y^2) X_k^{-3,2} X_k^{-3,-2} \right] \\ & - \frac{1}{32} b(-kn) \left[2(1-3x^2)^2 (X_k^{-3,0})^2 k\sqrt{1-e^2} + 9(1-x^2)^2 (X_k^{-3,-2})^2 \left(1 + \frac{k}{2}\sqrt{1-e^2}\right) \right. \\ & - 9(1-x^2)^2 (X_k^{-3,2})^2 \left(1 - \frac{k}{2}\sqrt{1-e^2}\right) - 6(1-3x^2)(1-x^2-2y^2) X_k^{-3,0} X_k^{-3,-2} \left(1 + k\sqrt{1-e^2}\right) \\ & \left. + 6(1-3x^2)(1-x^2-2y^2) X_k^{-3,0} X_k^{-3,2} (1-k\sqrt{1-e^2}) + 9\left((1-x^2)^2 - 8(1-x^2-y^2)y^2\right) X_k^{-3,2} X_k^{-3,-2} k\sqrt{1-e^2} \right] \\ & - \frac{3}{16} b(\omega - kn) \left[4(1-x^2)x^2 (X_k^{-3,0})^2 k\sqrt{1-e^2} + (1-x^2)(1-x)^2 (X_k^{-3,-2})^2 (2+k\sqrt{1-e^2}) \right. \\ & - (1-x^2)(1+x)^2 (X_k^{-3,2})^2 (2-k\sqrt{1-e^2}) + 4x(1-x)(1-x^2-2y^2) X_k^{-3,0} X_k^{-3,-2} (1+k\sqrt{1-e^2}) \\ & \left. + 4x(1+x)(1-x^2-2y^2) X_k^{-3,0} X_k^{-3,2} (1-k\sqrt{1-e^2}) \right. \\ & \left. - 2\left((1-x^2)^2 - 8(1-x^2-y^2)y^2\right) X_k^{-3,2} X_k^{-3,-2} k\sqrt{1-e^2} \right] \\ & - \frac{3}{64} b(2\omega - kn) \left[4(1-x^2)^2 (X_k^{-3,0})^2 k\sqrt{1-e^2} \right. \\ & \left. + (1-x)^4 (X_k^{-3,-2})^2 (2+k\sqrt{1-e^2}) - (1+x)^4 (X_k^{-3,2})^2 (2-k\sqrt{1-e^2}) \right. \\ & \left. + 4(1-x)^2 (1-x^2-2y^2) X_k^{-3,0} X_k^{-3,-2} (1+k\sqrt{1-e^2}) \right. \\ & \left. - 4(1+x)^2 (1-x^2-2y^2) X_k^{-3,0} X_k^{-3,2} (1-k\sqrt{1-e^2}) \right. \\ & \left. + 2\left((1-x^2)^2 - 8(1-x^2-y^2)y^2\right) X_k^{-3,2} X_k^{-3,-2} k\sqrt{1-e^2} \right] \left. \right\}, \quad (86) \end{aligned}$$

$$\begin{aligned}
\dot{\phi} = & -\frac{\mathcal{E}_0 e}{\sqrt{1-e^2}} \sum_{k=-\infty}^{+\infty} \left\{ \frac{3}{32} z a(-kn) \left[4x(1-3x^2) \left(X_k^{-3,0} \right)^2 + 3x(1-x^2) \left(\left(X_k^{-3,-2} \right)^2 + \left(X_k^{-3,2} \right)^2 \right) \right. \right. \\
& - 4x(2-3(x^2+y^2)) X_k^{-3,0} \left(X_k^{-3,-2} + X_k^{-3,2} \right) + 6x(1-x^2-4y^2) X_k^{-3,2} X_k^{-3,-2} \left. \right] \\
& - \frac{3}{16} z a(\omega - kn) \left[4x(1-2x^2) \left(X_k^{-3,0} \right)^2 - (1-x)^2(1+2x) \left(X_k^{-3,-2} \right)^2 + (1+x)^2(1-2x) \left(X_k^{-3,2} \right)^2 \right. \\
& + 2((1-x)(1-x-4x^2) - 2(1-2x)y^2) X_k^{-3,0} X_k^{-3,-2} \\
& - 2((1+x)(1+x-4x^2) - 2(1+2x)y^2) X_k^{-3,0} X_k^{-3,2} + 4x(1-x^2-4y^2) X_k^{-3,2} X_k^{-3,-2} \left. \right] \\
& + \frac{3}{32} z a(2\omega - kn) \left[4x(1-x^2) \left(X_k^{-3,0} \right)^2 + (1-x)^3 \left(X_k^{-3,-2} \right)^2 - (1+x)^3 \left(X_k^{-3,2} \right)^2 \right. \\
& + 2((1-x)^2(1+2x) - 2(1-x)y^2) X_k^{-3,0} X_k^{-3,-2} - 2((1+x)^2(1-2x) - 2(1+x)y^2) X_k^{-3,0} X_k^{-3,2} \\
& \left. + 2x(1-x^2-4y^2) X_k^{-3,2} X_k^{-3,-2} \right] \\
& + \frac{3}{32} y b(-kn) \left[3x(1-x^2) \left(\left(X_k^{-3,-2} \right)^2 - \left(X_k^{-3,2} \right)^2 \right) - 2x(5-3(x^2+2y^2)) X_k^{-3,0} \left(X_k^{-3,-2} - X_k^{-3,2} \right) \right] \\
& + \frac{3}{16} y b(\omega - kn) \left[4x^2 \left(X_k^{-3,0} \right)^2 + (1-x)^2(1+2x) \left(X_k^{-3,-2} \right)^2 + (1+x)^2(1-2x) \left(X_k^{-3,2} \right)^2 \right. \\
& - 4((1-x)(1-x^2) - (1-2x)y^2) X_k^{-3,0} X_k^{-3,-2} - 4((1+x)(1-x^2) - (1+2x)y^2) X_k^{-3,0} X_k^{-3,2} \\
& \left. + 2(3-3x^2-4y^2) X_k^{-3,2} X_k^{-3,-2} \right] \\
& + \frac{3}{32} y b(2\omega - kn) \left[4(1-x^2) \left(X_k^{-3,0} \right)^2 + (1-x)^3 \left(X_k^{-3,-2} \right)^2 + (1+x)^3 \left(X_k^{-3,2} \right)^2 \right. \\
& + 2(x(1-x)^2 - 2(1-x)y^2) X_k^{-3,0} X_k^{-3,-2} - 2(x(1+x)^2 + 2(1+x)y^2) X_k^{-3,0} X_k^{-3,2} \\
& \left. - 2(3-3x^2-4y^2) X_k^{-3,2} X_k^{-3,-2} \right] \left. \right\},
\end{aligned}$$

(87)

$$\begin{aligned}
e\dot{\omega}_a = & -\frac{\mathcal{E}_0}{e\sqrt{1-e^2}} \sum_{k=-\infty}^{+\infty} \left\{ \frac{3}{32} a(-kn) \left[2(x^2 - y^2 - 3x^2(x^2 - y^2)) e^2 (X_k^{-3,0})^2 \right. \right. \\
& + \frac{3}{2} \left((1-x^2)^2 (2+k(1-e^2)^{3/2}) - (x^2(1-x^2) + (3-5x^2-2y^2)y^2) e^2 \right) (X_k^{-3,-2})^2 \\
& + \frac{3}{2} \left((1-x^2)^2 (2-k(1-e^2)^{3/2}) - (x^2(1-x^2) + (3-5x^2-2y^2)y^2) e^2 \right) (X_k^{-3,2})^2 \\
& - 2((1-x^2(4-3x^2) - 2y^2(1-3x^2)) + (x^2-y^2)(1-3y^2) e^2) X_k^{-3,0} (X_k^{-3,-2} + X_k^{-3,2}) \\
& - (1-x^2(4-3x^2) - 2y^2(1-3x^2) + 4y^2(1-x^2-y^2)) X_k^{-3,0} (X_k^{-3,-2} - X_k^{-3,2}) k(1-e^2)^{3/2} \\
& + 3(2(1-x^2)^2 - 16y^2(1-x^2-y^2) + (y^2(5-6y^2) - x^2(1-x^2+3y^2)) e^2) X_k^{-3,2} X_k^{-3,-2} \\
& - 2(1-y^2-x^2(5-6x^2-3y^2)) X_k^{-3,0} (X_k^{-3,-1} + X_k^{-3,1}) e \\
& \left. + 3((1-3y^2+2y^4) - x^2(3-2x^2-5y^2)) (X_k^{-3,-2} + X_k^{-3,2}) (X_k^{-3,-1} + X_k^{-3,1}) e \right] \\
& - \frac{1}{8} a(\omega - kn) \left[2x(3x(1-x^2+y^2) e^2 + (1-x^2-2y^2) k(1-e^2)^{3/2}) (X_k^{-3,0})^2 \right. \\
& - \frac{3}{2} \left((1-x)^2(1-x^2) (2+k(1-e^2)^{3/2}) - (1-2y^2(1-y^2) - 3xy^2 - x^2(2-5y^2-x^2)) e^2 \right) (X_k^{-3,-2})^2 \\
& - \frac{3}{2} \left((1+x)^2(1-x^2) (2-k(1-e^2)^{3/2}) - (1-2y^2(1-y^2) + 3xy^2 - x^2(2-5y^2-x^2)) e^2 \right) (X_k^{-3,2})^2 \\
& + 2(3x^2(1-x^2-2y^2) + 3y^2(1+x^2-y^2) e^2 - x(2-2x^2-3y^2) k(1-e^2)^{3/2}) X_k^{-3,0} (X_k^{-3,-2} + X_k^{-3,2}) \\
& - (6x(1-x^2-2y^2) - 3x(2-2x^2-5y^2) e^2 \\
& \quad - (1-4y^2(1-y^2) + x^2(2-3x^2-2y^2)) k(1-e^2)^{3/2}) X_k^{-3,0} (X_k^{-3,-2} - X_k^{-3,2}) \\
& + 3(2(1-x^2)^2 - 16y^2(1-x^2-y^2) - (1-6y^2(1-y^2) + x^2(3y^2-x^2)) e^2) X_k^{-3,2} X_k^{-3,-2} \\
& + 6x^2(2-2x^2-y^2) X_k^{-3,0} (X_k^{-3,-1} + X_k^{-3,1}) e \\
& - 3(2y^2(1-y^2) - x(2-3y^2) + x^2(2+2x-2x^2-5y^2)) X_k^{-3,-2} (X_k^{-3,-1} + X_k^{-3,1}) e \\
& - 3(2y^2(1-y^2) + x(2-3y^2) + x^2(2-2x-2x^2-5y^2)) X_k^{-3,2} (X_k^{-3,-1} + X_k^{-3,1}) e \left. \right] \\
& + \frac{1}{32} a(2\omega - kn) \left[2(2x(1-x^2-2y^2) k(1-e^2)^{3/2} - 3(2-y^2-x^2(3-x^2+y^2)) e^2) (X_k^{-3,0})^2 \right. \\
& + \frac{3}{2} \left((1-x)^4 (2+k(1-e^2)^{3/2}) - (2-y^2(1+2y^2) - 6x(1-y^2) + x^2(5-5y^2-x^2)) e^2 \right) (X_k^{-3,-2})^2 \\
& + \frac{3}{2} \left((1+x)^4 (2-k(1-e^2)^{3/2}) - (2-y^2(1+2y^2) + 6x(1-y^2) + x^2(5-5y^2-x^2)) e^2 \right) (X_k^{-3,2})^2 \\
& + 2(3(1-2y^2-x^2(x^2+2y^2)) - 3(2-y^2(3-y^2) - x^2(1+y^2)) e^2 \\
& \quad - 2x(1-3y^2-2x^2) k(1-e^2)^{3/2}) X_k^{-3,0} (X_k^{-3,-2} + X_k^{-3,2}) \\
& - (12x(1-x^2-2y^2) - 6x(3-2x^2-5y^2) e^2 \\
& \quad - (3-2y^2(5-2y^2) - x^2(4+2y^2+3x^2)) k(1-e^2)^{3/2}) X_k^{-3,0} (X_k^{-3,-2} - X_k^{-3,2}) \\
& + 3(2(1-x^2)^2 - 16y^2(1-x^2-y^2) - (2-9y^2+6y^4-x^2(3+x^2-3y^2)) e^2) X_k^{-3,2} X_k^{-3,-2} \\
& - 6(1+y^2-x^2(3-2x^2-y^2)) X_k^{-3,0} (X_k^{-3,-1} + X_k^{-3,1}) e \\
& - 3(1-y^2(1+2y^2) - 2x(1-3y^2) - x^2(1-4x+2x^2+5y^2)) X_k^{-3,-2} (X_k^{-3,-1} + X_k^{-3,1}) e \\
& \left. - 3(1-y^2(1+2y^2) + 2x(1-3y^2) - x^2(1+4x+2x^2+5y^2)) X_k^{-3,2} (X_k^{-3,-1} + X_k^{-3,1}) e \right\}, \tag{88}
\end{aligned}$$

$$\begin{aligned}
e\dot{\omega}_b = & \frac{\mathcal{E}_0}{e\sqrt{1-e^2}} \sum_{k=-\infty}^{+\infty} \left\{ \frac{1}{16} yz b(-kn) \left[2(1-3x^2) (X_k^{-3,0})^2 k (1-e^2)^{3/2} \right. \right. \\
& - \frac{9}{2} (1-2x^2-y^2) e^2 \left((X_k^{-3,-2})^2 - (X_k^{-3,2})^2 \right) \\
& - 3(2(1-3x^2) - (1-3y^2)e^2) X_k^{-3,0} (X_k^{-3,-2} - X_k^{-3,2}) \\
& - 6(1-2x^2-y^2) X_k^{-3,0} (X_k^{-3,-2} + X_k^{-3,2}) k (1-e^2)^{3/2} \\
& + 18(1-x^2-2y^2) X_k^{-3,2} X_k^{-3,-2} k (1-e^2)^{3/2} \\
& \left. - 9(1-2x^2-y^2) (X_k^{-3,-1} + X_k^{-3,1}) (X_k^{-3,-2} - X_k^{-3,2}) e \right] \\
& - \frac{1}{8} yz b(\omega - kn) \left[2x(3e^2 - 2xk(1-e^2)^{3/2}) (X_k^{-3,0})^2 \right. \\
& - \frac{3}{2} (1+3x-4x^2-2y^2) e^2 (X_k^{-3,-2})^2 + \frac{3}{2} (1-3x-4x^2-2y^2) e^2 (X_k^{-3,2})^2 \\
& - 2(6x+3xe^2 + (1-4x^2-2y^2)k(1-e^2)^{3/2}) X_k^{-3,0} (X_k^{-3,-2} + X_k^{-3,2}) \\
& + 3(4x^2 + (1-2y^2)e^2 - 2xk(1-e^2)^{3/2}) X_k^{-3,0} (X_k^{-3,-2} - X_k^{-3,2}) \\
& + 3(4(1-x^2-2y^2)k(1-e^2)^{3/2} - 3xe^2) X_k^{-3,2} X_k^{-3,-2} - 6x X_k^{-3,0} (X_k^{-3,-1} + X_k^{-3,1}) e \\
& - 3(1+3x-4x^2-2y^2) X_k^{-3,-2} (X_k^{-3,-1} + X_k^{-3,1}) e \\
& \left. + 3(1-3x-4x^2-2y^2) X_k^{-3,2} (X_k^{-3,-1} + X_k^{-3,1}) e \right] \\
& - \frac{1}{16} yz b(2\omega - kn) \left[2((1+x^2)k(1-e^2)^{3/2} - 3xe^2) (X_k^{-3,0})^2 \right. \\
& - \frac{3}{2} (1-3x+2x^2+y^2) e^2 (X_k^{-3,-2})^2 + \frac{3}{2} (1+3x+2x^2+y^2) e^2 (X_k^{-3,2})^2 \\
& + 2(6x+3xe^2 - (1+2x^2+y^2)k(1-e^2)^{3/2}) X_k^{-3,0} (X_k^{-3,-2} + X_k^{-3,2}) \\
& - 3(2(1+x^2) + (1-y^2)e^2 - 2xk(1-e^2)^{3/2}) X_k^{-3,0} (X_k^{-3,-2} - X_k^{-3,2}) \\
& - 3(2(1-x^2-2y^2)k(1-e^2)^{3/2} - 3xe^2) X_k^{-3,2} X_k^{-3,-2} + 6x X_k^{-3,0} (X_k^{-3,-1} + X_k^{-3,1}) e \\
& - 3(1-3x+2x^2+y^2) X_k^{-3,-2} (X_k^{-3,-1} + X_k^{-3,1}) e \\
& \left. + 3(1+3x+2x^2+y^2) X_k^{-3,2} (X_k^{-3,-1} + X_k^{-3,1}) e \right] \left. \right\}, \tag{89}
\end{aligned}$$

where

$$\dot{\omega} = \dot{\omega}_a + \dot{\omega}_b, \tag{90}$$

and

$$\mathcal{E}_0 = n \left(\frac{m_0}{m} \right) \left(\frac{R}{a} \right)^5 = \frac{\mathcal{T}_0}{\beta n a^2}. \tag{91}$$

We note that for the \dot{e} and $e\dot{\omega}$ projections of the Laplace vector, all terms in the series appear combined with one of the following combinations of the Hansen coefficients: $X_k^{-3,m} X_k^{-3,m'}$ with $m \neq m'$, $e X_k^{-3,\pm 1} X_k^{-3,m}$, $e^2 (X_k^{-3,m})^2$, $k (X_k^{-3,0})^2$, or $(2 \mp k) (X_k^{-3,\pm 2})^2$. As a result, all these terms are proportional to e^2 for all values of k (Table 1), which suppresses the potential singularity at $e = 0$ introduced by the factor e^{-1} in their amplitudes. It also ensures that there is no problem with the terms in y and z if we are unable to accurately obtain \hat{e} from \mathbf{e} when $e \approx 0$ (Eq. (76)).

3.3 Orbital and spin evolution

The set of equations (77) and (85) allow us to track the evolution of the averaged system using the angular momentum and the Laplace vectors (Sect. 2.3). For a more intuitive description of the orbital and spin evolution, we can relate these vectors with the rotation and orbital elliptic elements. The eccentricity can be directly obtained from the Laplace vector,

$$e = \sqrt{\mathbf{e} \cdot \mathbf{e}}, \quad (92)$$

the semi-major axis from the orbital angular momentum (Eq. (1)),

$$a = \frac{\mathbf{G} \cdot \mathbf{G}}{\beta^2 \mu (1 - e^2)}, \quad (93)$$

and the rotation rate from the rotational angular momentum (Eq. (4)),

$$\omega = \frac{\sqrt{\mathbf{L} \cdot \mathbf{L}}}{C}. \quad (94)$$

The argument of the pericentre is given by expression (51), while the angle between the orbital and equatorial planes, can be obtained from both angular momentum vectors as

$$\cos \theta = \mathbf{k} \cdot \mathbf{s} = \frac{\mathbf{G} \cdot \mathbf{L}}{\sqrt{(\mathbf{G} \cdot \mathbf{G})(\mathbf{L} \cdot \mathbf{L})}}. \quad (95)$$

For a better comparison with previous studies, we can also obtain the evolution of all these quantities. The eccentricity and the argument of the pericentre evolution are already given by two projections of the Laplace vector, namely by \dot{e} (Eq. (86)) and $\dot{\varpi}$ (Eq. (90)), respectively:

$$\dot{e} = \dot{\mathbf{e}} \cdot \hat{\mathbf{e}}, \quad \text{and} \quad \dot{\varpi} = \dot{\mathbf{e}} \cdot (\mathbf{k} \times \hat{\mathbf{e}}) / e. \quad (96)$$

The semi-major axis evolution is given from expressions (19), (93) and (96),

$$\dot{a} = \frac{2 \mathbf{G} \cdot \mathbf{T}}{\beta^2 \mu (1 - e^2)} + \frac{2 a \mathbf{e} \cdot \dot{\mathbf{e}}}{(1 - e^2)} = \frac{2(T_1 + T_2 x - T_5 z)}{\beta n a \sqrt{1 - e^2}} + \frac{2 a e \dot{e}}{(1 - e^2)}, \quad (97)$$

or, making use of expressions (79), (80), (83), and (86), we have

$$\begin{aligned} \frac{\dot{a}}{a} = \mathcal{E}_0 \sum_{k=-\infty}^{+\infty} & \left\{ \frac{1}{16} k b (-kn) \left[2 (1 - 3x^2)^2 (X_k^{-3,0})^2 + \frac{9}{2} (1 - x^2)^2 \left((X_k^{-3,-2})^2 + (X_k^{-3,2})^2 \right) \right. \right. \\ & - 6 (1 - 3x^2) (1 - x^2 - 2y^2) X_k^{-3,0} (X_k^{-3,-2} + X_k^{-3,2}) + 9 \left((1 - x^2)^2 - 8 (1 - x^2 - y^2) y^2 \right) X_k^{-3,2} X_k^{-3,-2} \left. \right] \\ & + \frac{3}{8} k b (\omega - kn) \left[4 (1 - x^2) x^2 (X_k^{-3,0})^2 + (1 - x^2) (1 - x)^2 (X_k^{-3,-2})^2 + (1 - x^2) (1 + x)^2 (X_k^{-3,2})^2 \right. \\ & + 4x (1 - x) (1 - x^2 - 2y^2) X_k^{-3,0} X_k^{-3,-2} - 4x (1 + x) (1 - x^2 - 2y^2) X_k^{-3,0} X_k^{-3,2} \\ & \left. - 2 \left((1 - x^2)^2 - 8 (1 - x^2 - y^2) y^2 \right) X_k^{-3,2} X_k^{-3,-2} \right] \\ & + \frac{3}{32} k b (2\omega - kn) \left[4 (1 - x^2)^2 (X_k^{-3,0})^2 + (1 - x)^4 (X_k^{-3,-2})^2 + (1 + x)^4 (X_k^{-3,2})^2 \right. \\ & + 4 (1 - x)^2 (1 - x^2 - 2y^2) X_k^{-3,0} X_k^{-3,-2} + 4 (1 + x)^2 (1 - x^2 - 2y^2) X_k^{-3,0} X_k^{-3,2} \\ & \left. + 2 \left((1 - x^2)^2 - 8 (1 - x^2 - y^2) y^2 \right) X_k^{-3,2} X_k^{-3,-2} \right] \left. \right\}. \quad (98) \end{aligned}$$

For the rotation rate evolution, we have from expressions (20) and (94),

$$\dot{\omega} = -\frac{\mathbf{T} \cdot \mathbf{s}}{C} = -\frac{T_1 x + T_2 + T_4 y}{C}, \quad (99)$$

that is, using expressions (79), (80), and (82),

$$\begin{aligned} \dot{\omega} = & -\frac{T_0}{C} \sum_{k=-\infty}^{+\infty} \left\{ \frac{3}{16} b(\omega - kn) \left[(1-x)^2 (1-x^2) \left(X_k^{-3,-2} \right)^2 + (1+x)^2 (1-x^2) \left(X_k^{-3,2} \right)^2 \right. \right. \\ & - 2 \left((1-x^2)^2 - 8(1-x^2-y^2)y^2 \right) X_k^{-3,2} X_k^{-3,-2} + 4x^2 (1-x^2) \left(X_k^{-3,0} \right)^2 \\ & \left. \left. + 4x(1-x)(1-x^2-2y^2) X_k^{-3,0} X_k^{-3,-2} - 4x(1+x)(1-x^2-2y^2) X_k^{-3,0} X_k^{-3,2} \right] \right. \\ & + \frac{3}{32} b(2\omega - kn) \left[(1-x)^4 \left(X_k^{-3,-2} \right)^2 + (1+x)^4 \left(X_k^{-3,2} \right)^2 \right. \\ & + 2 \left((1-x^2)^2 - 8(1-x^2-y^2)y^2 \right) X_k^{-3,2} X_k^{-3,-2} + 4(1-x^2)^2 \left(X_k^{-3,0} \right)^2 \\ & \left. \left. + 4(1-x^2-2y^2)(1-x)^2 X_k^{-3,0} X_k^{-3,-2} + 4(1-x^2-2y^2)(1+x)^2 X_k^{-3,0} X_k^{-3,2} \right] \right\}. \end{aligned} \quad (100)$$

The obliquity (or inclination) evolution is given from expressions (19), (20) and (95),

$$\begin{aligned} \dot{\theta} = & \frac{\mathbf{T} \cdot \mathbf{k} - \mathbf{T} \cdot \mathbf{s} \cos \theta}{\sin \theta \sqrt{\mathbf{L} \cdot \mathbf{L}}} - \frac{\mathbf{T} \cdot \mathbf{s} - \mathbf{T} \cdot \mathbf{k} \cos \theta}{\sin \theta \sqrt{\mathbf{G} \cdot \mathbf{G}}} \\ = & \frac{T_1 \sin^2 \theta - T_4 xy - T_5 z}{C \omega \sin \theta} - \frac{T_2 \sin^2 \theta + T_4 y + T_5 xz}{\beta \sqrt{\mu a (1-e^2)} \sin \theta}. \end{aligned} \quad (101)$$

We observe that there are two distinct contributions to the evolution of this angle. When $|\mathbf{L}| \ll |\mathbf{G}|$, the evolution is dominated by the first term, and $\dot{\theta}$ is identified as a variation of the obliquity. This is, for instance, the case of a planet around a star. On the other hand, when $|\mathbf{L}| \gg |\mathbf{G}|$, the evolution is dominated by the second term, and $\dot{\theta}$ is recognised as a variation in the orbital inclination. This is, for instance, the case of a small satellite close to its planet. Previous studies often neglect one of these two contributions, and therefore, the evolution of this angle is incomplete.

Finally, we can also obtain the evolution of the precession angles, that is, the angular velocity of the longitude of the node, $\dot{\Omega}$, and the precession speed of the spin axis, $\dot{\psi}$. The line of nodes is aligned with the vector \mathbf{p} (Fig. 1) and thus

$$\dot{\Omega} = \frac{\dot{\mathbf{G}}}{|\mathbf{G}|} \cdot \mathbf{p} = \frac{\mathbf{T} \cdot \mathbf{p}}{|\mathbf{G}|} = \frac{T_3 \sin^2 \theta - T_4 z + T_5 xy}{\beta \sqrt{\mu a (1-e^2)} \sin \theta}, \quad (102)$$

$$\dot{\psi} = \frac{\dot{\mathbf{L}}}{|\mathbf{L}|} \cdot \mathbf{p} = -\frac{\mathbf{T} \cdot \mathbf{p}}{|\mathbf{L}|} = -\frac{T_3 \sin^2 \theta - T_4 z + T_5 xy}{C \omega \sin \theta}. \quad (103)$$

3.4 Energy dissipation

The total energy released inside the body due to tides is given by

$$\dot{E} = -(\dot{E}_{\text{orb}} + \dot{E}_{\text{rot}}), \quad (104)$$

where

$$E_{\text{orb}} = -\frac{\beta \mu}{2a} \quad \text{and} \quad E_{\text{rot}} = \frac{\boldsymbol{\omega} \cdot \mathbf{L}}{2} \quad (105)$$

are the orbital energy, and the rotational energy, respectively. Then

$$\dot{E}_{\text{orb}} = \frac{\beta \mu}{2a^2} \dot{a} \quad \text{and} \quad \dot{E}_{\text{rot}} = C \omega \dot{\omega}, \quad (106)$$

where \dot{a} and $\dot{\omega}$ are given by expressions (98) and (100), respectively.

4 Average over the argument of the pericentre

Although we usually have $\overline{\dot{\varpi}} \ll n$, the argument of the pericentre can often also be considered a fast varying angle when compared to the secular tidal evolution of the remaining spin and orbital elements. This is particularly true when additional sources of precession are taken into account in the problem, such as the rotational deformation, general relativity corrections and additional perturbing bodies in the system. As a result, we can perform a second average of the equations of motion, this time over the angle ϖ . Adopting again as example the last term in the \mathbf{s} component of the tidal torque, we have (Eq. (71))

$$\left\langle -\frac{3\mathcal{G}m_0}{r^3} I_{23} \hat{x}_1 \hat{x}_3 \right\rangle_{M, \varpi} = \frac{3\mathcal{G}m_0^2 R^5}{16a^6} \sin^2 \theta \sum_{k=-\infty}^{+\infty} b(\omega - kn) \left[(1-x) \left(X_k^{-3,-2} \right)^2 + (1+x) \left(X_k^{-3,2} \right)^2 \right], \quad (107)$$

which considerably simplifies the expression of the equations of motion. In this particular case, we note that there is no longer the contribution from $a(\omega - kn)$.

Another simplification is that we do not need to follow the evolution of the Laplace vector anymore. Indeed, the pericentre is no longer defined when we average over ϖ , and the only projection of interest is the one giving the evolution of the eccentricity, $\hat{\mathbf{e}}$. Therefore, the equations of motion in this simplified case can be given by the torque together with $\dot{\mathbf{e}}$. Alternatively, we prefer to use the evolution of the orbital energy, since it can be obtained directly from the potential energy (Eq. (7)) and thus provides a simpler expression (from which we can later easily derive $\dot{\mathbf{e}}$).

4.1 Tidal torque

When we average the tidal torque (Eq. (77)) over ϖ , the projections that depend on the Laplace vector average to zero and thus

$$\langle \mathbf{T} \rangle_{M, \varpi} = \bar{T}_1 \mathbf{k} + \bar{T}_2 \mathbf{s} + \bar{T}_3 \mathbf{k} \times \mathbf{s}, \quad (108)$$

with

$$\begin{aligned} \bar{T}_1 = -\mathcal{T}_0 \sum_{k=-\infty}^{+\infty} & \left\{ \frac{9}{32} b(-kn) \left[(1-x^2) \left(\left(X_k^{-3,-2} \right)^2 - \left(X_k^{-3,2} \right)^2 \right) \right] \right. \\ & + \frac{3}{16} b(\omega - kn) \left[4x^3 \left(X_k^{-3,0} \right)^2 + (1-x)^2 (2+x) \left(X_k^{-3,-2} \right)^2 - (1+x)^2 (2-x) \left(X_k^{-3,2} \right)^2 \right] \\ & \left. + \frac{3}{32} b(2\omega - kn) \left[4x(1-x^2) \left(X_k^{-3,0} \right)^2 + (1-x)^3 \left(X_k^{-3,-2} \right)^2 - (1+x)^3 \left(X_k^{-3,2} \right)^2 \right] \right\}, \end{aligned} \quad (109)$$

$$\begin{aligned} \bar{T}_2 = \mathcal{T}_0 \sum_{k=-\infty}^{+\infty} & \left\{ \frac{9}{32} b(-kn) \left[x(1-x^2) \left(\left(X_k^{-3,-2} \right)^2 - \left(X_k^{-3,2} \right)^2 \right) \right] \right. \\ & + \frac{3}{16} b(\omega - kn) \left[4x^2 \left(X_k^{-3,0} \right)^2 + (1-x)^2 (1+2x) \left(X_k^{-3,-2} \right)^2 + (1+x)^2 (1-2x) \left(X_k^{-3,2} \right)^2 \right] \\ & \left. + \frac{3}{32} b(2\omega - kn) \left[4(1-x^2) \left(X_k^{-3,0} \right)^2 + (1-x)^3 \left(X_k^{-3,-2} \right)^2 + (1+x)^3 \left(X_k^{-3,2} \right)^2 \right] \right\}, \end{aligned} \quad (110)$$

$$\begin{aligned}
\bar{T}_3 = -\mathcal{T}_0 \sum_{k=-\infty}^{+\infty} & \left\{ \frac{3}{32} x a(-kn) \left[4(1-3x^2) \left(X_k^{-3,0} \right)^2 + 3(1-x^2) \left(\left(X_k^{-3,-2} \right)^2 + \left(X_k^{-3,2} \right)^2 \right) \right] \right. \\
& - \frac{3}{16} a(\omega - kn) \left[4x(1-2x^2) \left(X_k^{-3,0} \right)^2 - (1-x)^2(1+2x) \left(X_k^{-3,-2} \right)^2 + (1+x)^2(1-2x) \left(X_k^{-3,2} \right)^2 \right] \\
& \left. + \frac{3}{32} a(2\omega - kn) \left[4x(1-x^2) \left(X_k^{-3,0} \right)^2 + (1-x)^3 \left(X_k^{-3,-2} \right)^2 - (1+x)^3 \left(X_k^{-3,2} \right)^2 \right] \right\}. \tag{111}
\end{aligned}$$

Boué et al (2016)¹ obtained an equivalent expression for the double averaged tidal torque (Eq.(108)). However, they only consider the contribution to the spin evolution (Eq. (20)), while here, we also apply the torque to the orbital evolution (Eq. (19)). Moreover, to obtain the complete tidal evolution we additionally need to consider the evolution of the orbital energy (Eq. (113)).

4.2 Orbital energy

The evolution of the orbital energy is obtained from the work of the tidal force \mathbf{F} (Eq. (15)) as

$$\dot{E}_{\text{orb}} = \langle \mathbf{F} \cdot \dot{\mathbf{r}} \rangle_{M, \varpi} = - \left\langle \frac{\partial U}{\partial t} \right\rangle_{M, \varpi}. \tag{112}$$

The first approach provides the Hansen coefficients in the format $X_k^{-4,m}$, which can be put into the format $X_k^{-3,m}$ using the relations provided in appendix A. The second approach is easier to compute and already provides the Hansen coefficients in the format $X_k^{-3,m}$. Then,

$$\begin{aligned}
\dot{E}_{\text{orb}} = n \mathcal{T}_0 \sum_{k=-\infty}^{+\infty} & \left\{ \frac{1}{64} k b(-kn) \left[4(1-3x^2)^2 \left(X_k^{-3,0} \right)^2 + 9(1-x^2)^2 \left(\left(X_k^{-3,-2} \right)^2 + \left(X_k^{-3,2} \right)^2 \right) \right] \right. \\
& + \frac{3}{16} k b(\omega - kn) (1-x^2) \left[4x^2 \left(X_k^{-3,0} \right)^2 + (1-x)^2 \left(X_k^{-3,-2} \right)^2 + (1+x)^2 \left(X_k^{-3,2} \right)^2 \right] \\
& \left. + \frac{3}{64} k b(2\omega - kn) \left[4(1-x^2)^2 \left(X_k^{-3,0} \right)^2 + (1-x)^4 \left(X_k^{-3,-2} \right)^2 + (1+x)^4 \left(X_k^{-3,2} \right)^2 \right] \right\}. \tag{113}
\end{aligned}$$

4.3 Orbital and spin evolution

The set of equations (108) and (113) allow us to track the evolution of the averaged system using the angular momentum vectors and the orbital energy. As in Sect. 3.3, we can relate these quantities with the orbital and spin parameters. The semi-major axis is directly given from the orbital energy

$$a = -\frac{\beta\mu}{2E_{\text{orb}}}, \tag{114}$$

and the eccentricity from the orbital angular momentum (Eq. (1))

$$e = \sqrt{1 - \frac{\mathbf{G} \cdot \mathbf{G}}{\beta^2 \mu a}}. \tag{115}$$

The rotation rate, ω , is obtained from the rotational angular momentum (Eq. (94)), and the angle between the orbital and equatorial planes, θ , from both angular momentum vectors (Eq. (95)).

¹ Note that the $b(\sigma)$ functions have a slightly different definition. In Boué et al (2016) it is defined as the imaginary part of $\hat{k}_2(\sigma)$, while in our case it is defined as the opposite of it (Eq. (54)).

As in Sect. 3.3, we can also obtain the explicit evolution of all these quantities. The semi-major axis evolution is given from expression (113)

$$\dot{a} = \frac{2a^2}{\beta\mu} \dot{E}_{\text{orb}} , \quad (116)$$

while the eccentricity evolution can be computed from expressions (108), (115) and (116) as

$$\dot{e} = \frac{1-e^2}{2ae} \dot{a} - \frac{\mathbf{G} \cdot \mathbf{T}}{\beta^2 \mu a e} = \frac{\sqrt{1-e^2}}{\beta n a^2 e} \left(\frac{\sqrt{1-e^2}}{n} \dot{E}_{\text{orb}} - \bar{T}_1 - \bar{T}_2 x \right) , \quad (117)$$

that is, using expressions (109), (110), and (113),

$$\begin{aligned} \dot{e} = \varepsilon_0 \frac{\sqrt{1-e^2}}{e} \sum_{k=-\infty}^{+\infty} & \left\{ \frac{1}{64} b(-kn) \left[4(1-3x^2)^2 (X_k^{-3,0})^2 k\sqrt{1-e^2} \right. \right. \\ & + 9(1-x^2)^2 (X_k^{-3,-2})^2 (2+k\sqrt{1-e^2}) - 9(1-x^2)^2 (X_k^{-3,2})^2 (2-k\sqrt{1-e^2}) \left. \right] \\ & + \frac{3}{16} b(\omega - kn) \left[4(1-x^2) x^2 (X_k^{-3,0})^2 k\sqrt{1-e^2} \right. \\ & + (1-x^2)(1-x)^2 (X_k^{-3,-2})^2 (2+k\sqrt{1-e^2}) - (1-x^2)(1+x)^2 (X_k^{-3,2})^2 (2-k\sqrt{1-e^2}) \left. \right] \\ & + \frac{3}{64} b(2\omega - kn) \left[4(1-x^2)^2 (X_k^{-3,0})^2 k\sqrt{1-e^2} \right. \\ & \left. \left. + (1-x)^4 (X_k^{-3,-2})^2 (2+k\sqrt{1-e^2}) - (1+x)^4 (X_k^{-3,2})^2 (2-k\sqrt{1-e^2}) \right] \right\} . \end{aligned} \quad (118)$$

For the rotation rate evolution, we have from expressions (20) and (94),

$$\dot{\omega} = -\frac{\mathbf{T} \cdot \mathbf{s}}{C} = -\frac{\bar{T}_1 x + \bar{T}_2}{C} , \quad (119)$$

that is, using expressions (109) and (110)

$$\begin{aligned} \dot{\omega} = -\frac{\mathcal{T}_0}{C} \sum_{k=-\infty}^{+\infty} & \left\{ \frac{3}{16} b(\omega - kn) (1-x^2) \left[4x^2 (X_k^{-3,0})^2 + (1-x)^2 (X_k^{-3,-2})^2 + (1+x)^2 (X_k^{-3,2})^2 \right] \right. \\ & \left. + \frac{3}{32} b(2\omega - kn) \left[4(1-x^2)^2 (X_k^{-3,0})^2 + (1-x)^4 (X_k^{-3,-2})^2 + (1+x)^4 (X_k^{-3,2})^2 \right] \right\} . \end{aligned} \quad (120)$$

The obliquity (or inclination) evolution is given from expressions (101) and (108),

$$\dot{\theta} = \left(\frac{\bar{T}_1}{C\omega} - \frac{\bar{T}_2}{\beta\sqrt{\mu a(1-e^2)}} \right) \sin \theta . \quad (121)$$

Finally, for the angular velocity of the longitude of the node and for the precession speed of the spin axis, we get from expressions (102), (103) and (108), respectively,

$$\dot{\Omega} = \frac{\mathbf{T} \cdot (\mathbf{k} \times \mathbf{s})}{|\mathbf{G}| \sin \theta} = \frac{\bar{T}_3 \sin \theta}{\beta\sqrt{\mu a(1-e^2)}} , \quad (122)$$

$$\dot{\psi} = -\frac{\mathbf{T} \cdot (\mathbf{k} \times \mathbf{s})}{|\mathbf{L}| \sin \theta} = -\frac{\bar{T}_3 \sin \theta}{C\omega} . \quad (123)$$

4.4 Energy dissipation

The total energy released inside the body due to tides is given by expressions (104) and (106). When we average over the argument of the pericentre, by combining expressions (113) and (120) we obtain for the total energy dissipated

$$\begin{aligned} \dot{E} = \mathcal{T}_0 \sum_{k=-\infty}^{+\infty} & \left\{ \frac{1}{64} (-kn) b(-kn) \left[4(1-3x^2)^2 (X_k^{-3,0})^2 + 9(1-x^2)^2 \left((X_k^{-3,-2})^2 + (X_k^{-3,2})^2 \right) \right] \right. \\ & + \frac{3}{16} (\omega - kn) b(\omega - kn) (1-x^2) \left[4x^2 (X_k^{-3,0})^2 + (1-x)^2 (X_k^{-3,-2})^2 + (1+x)^2 (X_k^{-3,2})^2 \right] \\ & \left. + \frac{3}{64} (2\omega - kn) b(2\omega - kn) \left[4(1-x^2)^2 (X_k^{-3,0})^2 + (1-x)^4 (X_k^{-3,-2})^2 + (1+x)^4 (X_k^{-3,2})^2 \right] \right\}. \end{aligned} \quad (124)$$

5 Planar case

The final outcome of tidal dissipation is the alignment of the spin axis with the normal to the orbit (Hut, 1980; Adams and Bloch, 2015). Therefore, in order to simplify the equations of motion, many works assume that this alignment is always present, that is, the motion is planar ($\theta = 0$). Indeed, in this case we have $\mathbf{k} = \mathbf{s}$ and thus (Eq. (76)):

$$x = 1, \quad y = 0, \quad \text{and} \quad z = 0. \quad (125)$$

5.1 Tidal torque

Using the simplifications (125) in expressions (82) and (83) yields $T_4 = T_5 = 0$. In addition, since we also have $\mathbf{k} \times \mathbf{s} = 0$, we get for the average tidal torque (Eq. (77))

$$\langle \mathbf{T} \rangle_M = (T_1 + T_2) \mathbf{k} = T_s \mathbf{k}, \quad (126)$$

with

$$T_s = \mathcal{T}_0 \sum_{k=-\infty}^{+\infty} \frac{3}{2} b(2\omega - kn) (X_k^{-3,2})^2. \quad (127)$$

We note that, since $y = z = 0$, the expression of the tidal torque is the same whether we perform a single average over the mean anomaly (Eq. (77)) or if we additionally average over the argument of the pericentre (Eq. (108)).

5.2 Laplace vector

Using the simplifications (125) in expression (87) yields $\dot{\phi} = 0$. The averaged Laplace vector then becomes (Eq. (85))

$$\dot{\mathbf{e}} = \dot{e} \hat{\mathbf{e}} + \dot{\varpi} \mathbf{k} \times \mathbf{e}, \quad (128)$$

with

$$\dot{e} = \varepsilon_0 \frac{\sqrt{1-e^2}}{4e} \sum_{k=-\infty}^{+\infty} \left\{ b(-kn) (X_k^{-3,0})^2 k \sqrt{1-e^2} - 3b(2\omega - kn) (X_k^{-3,2})^2 (2 - k \sqrt{1-e^2}) \right\}, \quad (129)$$

and

$$\begin{aligned} \dot{\omega} = \frac{\mathcal{E}_0}{e^2\sqrt{1-e^2}} \sum_{k=-\infty}^{+\infty} & \left\{ \frac{3}{16} a(-kn) \left[2e^2 (X_k^{-3,0})^2 + e^2 X_k^{-3,0} (X_k^{-3,-2} + X_k^{-3,2}) + 2e X_k^{-3,0} (X_k^{-3,-1} + X_k^{-3,1}) \right] \right. \\ & - \frac{1}{16} a(2\omega - kn) \left[(12(2-k(1-e^2)^{3/2}) - 9e^2) (X_k^{-3,2})^2 + 3e^2 X_k^{-3,2} X_k^{-3,-2} \right. \\ & \left. \left. + (4k(1-e^2)^{3/2} - 6e^2) X_k^{-3,0} X_k^{-3,2} + 6e X_k^{-3,2} (X_k^{-3,-1} + X_k^{-3,1}) \right] \right\}. \end{aligned} \quad (130)$$

We note that in the planar case, \dot{e} only depends on $b(\sigma)$, and $\dot{\omega}$ only depends on $a(\sigma)$. Moreover, the expression of \dot{e} does not change if we further average over the argument of the pericentre.

5.3 Orbital and spin evolution

For the semi-major axis, we have from expressions (97), (127) and (129),

$$\frac{\dot{a}}{a} = \mathcal{E}_0 \sum_{k=-\infty}^{+\infty} \frac{k}{2} \left[b(-kn) (X_k^{-3,0})^2 + 3b(2\omega - kn) (X_k^{-3,2})^2 \right], \quad (131)$$

while for the rotation rate, we get from expressions (99) and (127),

$$\dot{\omega} = -\frac{\mathcal{T}_0}{C} \sum_{k=-\infty}^{+\infty} \frac{3}{2} b(2\omega - kn) (X_k^{-3,2})^2. \quad (132)$$

Again, these expressions do not change if we further average over the argument of the pericentre. As expected, the evolution of the obliquity (or inclination) is simply given by $\dot{\theta} = 0$ (Eq. (101)), since $T_4 = T_5 = 0$ and $\sin \theta = 0$, that is, the motion remains planar.

5.4 Energy dissipation

The orbital and rotational energy variations can be obtained from expression (106) together with expressions (131) and (132), respectively

$$\dot{E}_{\text{orb}} = \mathcal{T}_0 \sum_{k=-\infty}^{+\infty} \frac{kn}{4} \left[b(-kn) (X_k^{-3,0})^2 + 3b(2\omega - kn) (X_k^{-3,2})^2 \right], \quad (133)$$

$$\dot{E}_{\text{rot}} = -\mathcal{T}_0 \sum_{k=-\infty}^{+\infty} \frac{3\omega}{2} b(2\omega - kn) (X_k^{-3,2})^2. \quad (134)$$

The total energy released inside the body due to tides is then (Eq. (104))

$$\dot{E} = \mathcal{T}_0 \sum_{k=-\infty}^{+\infty} \frac{1}{4} \left[(-kn) b(-kn) (X_k^{-3,0})^2 + 3(2\omega - kn) b(2\omega - kn) (X_k^{-3,2})^2 \right]. \quad (135)$$

ℓ	m	$\bar{X}_0^{-\ell,m}(e)$	ℓ	m	$\bar{X}_0^{-\ell,m}(e)$
6	0	$1 + 3e^2 + \frac{3}{8}e^4$	8	0	$1 + \frac{15}{2}e^2 + \frac{45}{8}e^4 + \frac{5}{16}e^6$
6	1	$2e(1 + \frac{3}{4}e^2)$	8	1	$3e(1 + \frac{5}{2}e^2 + \frac{5}{8}e^4)$
6	2	$\frac{3}{2}e^2(1 + \frac{1}{6}e^2)$	8	2	$\frac{15}{4}e^2(1 + e^2 + \frac{1}{16}e^4)$
6	3	$\frac{1}{2}e^3$	8	3	$\frac{5}{2}e^3(1 + \frac{3}{8}e^2)$
6	4	$\frac{1}{16}e^4$	8	4	$\frac{15}{16}e^4(1 + \frac{1}{10}e^2)$
9	0	$1 + \frac{21}{2}e^2 + \frac{105}{8}e^4 + \frac{35}{16}e^6$	10	0	$1 + 14e^2 + \frac{105}{4}e^4 + \frac{35}{4}e^6 + \frac{35}{128}e^8$
9	2	$\frac{21}{4}e^2(1 + \frac{5}{3}e^2 + \frac{5}{16}e^4)$	10	2	$7e^2(1 + \frac{5}{2}e^2 + \frac{15}{16}e^4 + \frac{1}{32}e^6)$
9	4	$\frac{35}{16}e^4(1 + \frac{3}{10}e^2)$	10	4	$\frac{35}{8}e^4(1 + \frac{3}{5}e^2 + \frac{1}{40}e^4)$

Table 2 Complete expression of the Hansen coefficients $X_0^{-\ell,m} = \bar{X}_0^{-\ell,m}/(1-e^2)^{\ell-3/2}$ (Eq. (139)), where $\bar{X}_0^{-\ell,m}$ is the polynomial part (see also [Laskar and Boué, 2010](#), Table A.1)).

6 Linear model

In Sect. 2.7, we present the tidal models most commonly used in the literature, and how they can be expressed in terms of the second Love number, $\hat{k}_2(\sigma)$. The linear or weak friction model is widely used because it is an approximation of any viscoelastic model for small relaxation times ($\sigma\tau \ll 1$) and provides simple expressions for the equations of motion that are valid for any eccentricity value. Indeed, since $a(\sigma)$ is constant and $b(\sigma) \propto \sigma$ (Eq. (60)), the sum of the Hansen coefficients products can be evaluated as (see appendix B):

$$\sum_{k=-\infty}^{+\infty} X_k^{-3,m} X_k^{-3,n} = X_0^{-6,m-n}, \quad (136)$$

$$\sum_{k=-\infty}^{+\infty} k X_k^{-3,m} X_k^{-3,n} = \frac{\sqrt{1-e^2}}{2} (m+n) X_0^{-8,m-n}, \quad (137)$$

$$\begin{aligned} \sum_{k=-\infty}^{+\infty} k^2 X_k^{-3,m} X_k^{-3,n} &= 9 \left(2X_0^{-9,m-n} - X_0^{-8,m-n} \right) \\ &+ \left(\frac{3}{8} (m-n)^2 + mn - 9 \right) (1-e^2) X_0^{-10,m-n}, \end{aligned} \quad (138)$$

where the coefficients $X_0^{-\ell,m}$ can be obtained as exact functions of the eccentricity (Eq. (49))

$$\begin{aligned} X_0^{-\ell,m}(e) &= \frac{1}{2\pi} \int_{-\pi}^{\pi} \left(\frac{a}{r} \right)^\ell e^{imv} dM = \frac{1}{\pi(1-e^2)^{\ell-3/2}} \int_0^\pi (1+e \cos v)^{\ell-2} \cos(mv) dv \\ &= \frac{1}{(1-e^2)^{\ell-3/2}} \sum_{k=0}^{(\ell-m-2)/2} \frac{(\ell-2)!}{k!(m+k)!(\ell-2-m-2k)!} \left(\frac{e}{2} \right)^{m+2k}. \end{aligned} \quad (139)$$

We provide the explicit expression of all needed $X_0^{-\ell,m}(e)$ coefficients in Table 2. The equations of motion that we obtain here are in perfect agreement with those derived in [Correia \(2009\)](#) and [Correia et al \(2011\)](#) using a different approach, and so for clearness reasons we keep the exact same notations for the eccentricity functions.

6.1 Average over the mean anomaly

6.1.1 Tidal torque

The averaged tidal torque is given by expression (77). In the linear approximation, the coefficients $T_3 = T_5 = 0$, and thus, we obtain

$$\begin{aligned} \langle \mathbf{T} \rangle_M = \mathcal{K}_t \left[\left(\sqrt{1-e^2} f_4(e) \frac{\omega}{2n} \cos \theta - f_2(e) \right) \mathbf{k} + \left(f_1(e) - \frac{1}{2} \sqrt{1-e^2} f_4(e) \right) \frac{\omega}{n} \mathbf{s} \right. \\ \left. + \left(\sqrt{1-e^2} f_4(e) - f_1(e) \right) \frac{\omega}{n} (\hat{\mathbf{e}} \cdot \mathbf{s}) \hat{\mathbf{e}} \right], \end{aligned} \quad (140)$$

with

$$f_1(e) = X_0^{-6,0}(e) = \frac{1 + 3e^2 + \frac{3}{8}e^4}{(1-e^2)^{9/2}}, \quad (141)$$

$$f_2(e) = \sqrt{1-e^2} X_0^{-8,0}(e) = \frac{1 + \frac{15}{2}e^2 + \frac{45}{8}e^4 + \frac{5}{16}e^6}{(1-e^2)^6}, \quad (142)$$

$$f_4(e) = \frac{X_0^{-6,0}(e) - X_0^{-6,2}(e)}{\sqrt{1-e^2}} = \frac{1 + \frac{3}{2}e^2 + \frac{1}{8}e^4}{(1-e^2)^5}, \quad (143)$$

and

$$\mathcal{K}_t = 3 \mathcal{T}_0 k_f n \Delta t = k_f \frac{3\mathcal{G}m_0^2 R^5}{a^6} n \Delta t. \quad (144)$$

6.1.2 Laplace vector

The averaged Laplace vector is given by expression (85). In the linear approximation, we obtain

$$\langle \dot{\mathbf{e}} \rangle_M = \mathcal{K}_e \left[\left(11 f_4(e) \frac{\omega}{2n} \cos \theta - 9 f_5(e) \right) \mathbf{e} - f_4(e) \frac{\omega}{2n} (\mathbf{e} \cdot \mathbf{s}) \mathbf{k} \right] + k_f \mathcal{E}_0 \frac{15}{2} f_4(e) \mathbf{k} \times \mathbf{e}, \quad (145)$$

with

$$f_5(e) = X_0^{-8,0}(e) - X_0^{-8,2}(e) = \frac{1 + \frac{15}{4}e^2 + \frac{15}{8}e^4 + \frac{5}{64}e^6}{(1-e^2)^{13/2}}, \quad (146)$$

and

$$\mathcal{K}_e = 3 \mathcal{E}_0 k_f n \Delta t = \frac{\mathcal{K}_t}{\beta n a^2} = k_f \frac{3\mathcal{G}m_0^2 R^5}{\beta a^8} \Delta t. \quad (147)$$

6.1.3 Orbital evolution

The evolution of the eccentricity and the argument of the pericentre in the linear approximation are already given by the first and third terms of the Laplace vector (Eq. (145)), respectively. For the semi-major axis, we have from expression (97)

$$\frac{\dot{a}}{a} = 2 \mathcal{K}_e \left[f_2(e) \frac{\omega}{n} \cos \theta - f_3(e) \right], \quad (148)$$

with

$$f_3(e) = 6X_0^{-9,0}(e) - 3X_0^{-8,0}(e) - 2(1-e^2)X_0^{-10,0}(e) = \frac{1 + \frac{31}{2}e^2 + \frac{255}{8}e^4 + \frac{185}{16}e^6 + \frac{25}{64}e^8}{(1-e^2)^{15/2}}. \quad (149)$$

6.2 Average over the argument of the pericentre

The eccentricity evolution (Eq. (145), first term) and the semi-major axis evolution (Eq. (148)) do not depend on the pericentre. In addition, the evolution of the pericentre (Eq. (145), last term) does not depend on the dissipation (Δt), and therefore evolves on a shorter timescale than the orbit. As a result, we can further average the equations of motion over the argument of the pericentre in order to get simpler expressions for the torque and spin evolution.

6.2.1 Tidal torque

The averaged tidal torque is now given by expression (108). In the linear approximation, it becomes

$$\langle \mathbf{T} \rangle_{M, \varpi} = \mathcal{K}_t \left[f_1(e) \frac{\omega}{2n} (\mathbf{s} + \cos \theta \mathbf{k}) - f_2(e) \mathbf{k} \right]. \quad (150)$$

6.2.2 Spin evolution

For the rotation rate, we get from expression (119)

$$\dot{\omega} = -\frac{\mathcal{K}_t}{C} \left[f_1(e) \frac{\omega}{2n} (1 + \cos^2 \theta) - f_2(e) \cos \theta \right], \quad (151)$$

and for the obliquity (or inclination) evolution we have from expression (121),

$$\dot{\theta} = \frac{\mathcal{K}_t}{C\omega} \left[f_1(e) \frac{\omega}{2n} \cos \theta - f_2(e) \right] \sin \theta - \frac{\mathcal{K}_e}{\sqrt{1-e^2}} f_1(e) \frac{\omega}{2n} \sin \theta. \quad (152)$$

6.3 Energy dissipation

The orbital and rotational energy variations can be obtained from expression (106) together with expressions (148) and (151), respectively. The total energy released inside the body due to tides is then (Eq. (104))

$$\dot{E} = n \mathcal{K}_t \left[\frac{1}{2} f_1(e) \left(\frac{\omega}{n} \right)^2 (1 + \cos^2 \theta) - 2 f_2(e) \frac{\omega}{n} \cos \theta + f_3(e) \right]. \quad (153)$$

7 Conclusion

In this paper, we revisit the tidal evolution of a body disturbed by a point mass companion. We derive the equations of motion in a vectorial formalism, where the basis depend only on the unit vectors of the spin and orbital angular momenta and on the Laplace unit vector. These vectors are related to the spin and orbital quantities, thus easy to obtain and independent of the chosen frame. We provide the expressions of the equations of motion for a single average over the mean anomaly, and also for an additional average over the argument of the pericentre. We show that in both cases, the equations depend only on series of Hansen coefficients, that are widely used in celestial mechanics. Our method is valid for any rheological model, which appears in the equations of motion through the second Love number.

In our model, we use the quadrupolar approximation to obtain the tidal potential (Eq. (6)), that is, we neglect terms in $(R/r)^3$. This approximation is usually suitable to study the long-term evolution of a large variety of systems, such as planet-satellite, planet-star or stellar binaries. However, for extremely close-in bodies with very asymmetric shapes, such as Phobos (the main

satellite of Mars) or binary asteroids, a high precision model of its tidal dynamics may require to include octupole or higher order terms in the tidal potential, as well as the knowledge of higher degree Love numbers (e.g., [Bills et al, 2005](#); [Taylor and Margot, 2010](#)).

In a more general two body problem, both bodies are expected to undergo tidal evolution. As long as we keep the quadrupolar approximation, the cross terms of interaction can be neglected (e.g., [Boué and Laskar, 2009](#)). As a result, we only need to take into account a second contribution to the potential energy (Eq. (7)), where m_0 is replaced by m , and \mathcal{I} is replaced by \mathcal{I}_0 (which pertains to the body with mass m_0). Therefore, we get additional similar expressions for the tidal force (Eq. (15)) and for the torque (Eq. (21)), where $(\mathbf{p}, \mathbf{q}, \mathbf{s})$ are replaced by $(\mathbf{p}_0, \mathbf{q}_0, \mathbf{s}_0)$ as they now also correspond to the body with mass m_0 . The equations of motion for the spin of m_0 are thus analogous to those for m (Eq. (20)), while for the equations of motion for the orbit (Eqs. (19) and (22)) we only need to add the contributions from the two bodies.

The vectorial formalism presented in this paper is well suited to study the long-term evolution of celestial bodies. In addition to tidal effects, we usually need to consider the rotational deformation and general relativity corrections (e.g., [Correia et al, 2011](#)). For multi-body systems, the secular interactions can be obtained either by developing the perturbing functions in terms of Legendre polynomials, suited for hierarchical systems (e.g., [Correia et al, 2016](#)), or in terms of Laplace coefficients, suited for non-resonant compact systems (e.g., [Boué and Fabrycky, 2014](#)).

Acknowledgements We thank G. Boué for discussions. We are grateful to two anonymous referees for their insightful comments. This work was supported by CFisUC (UIDB/04564/2020 and UIDP/04564/2020), GRAVITY (PTDC/FIS-AST/7002/2020), PHOBOS (POCI-01-0145-FEDER-029932), and ENGAGE SKA (POCI-01-0145-FEDER-022217), funded by COMPETE 2020 and FCT, Portugal.

A Hansen coefficients relations

From the definition of the Hansen coefficients (Eq. (48)), a number of recurrence relations can be obtained. In this work we use the following ones (e.g., [Challe and Laclaverie, 1969](#); [Giacaglia, 1976](#)):

$$X_k^{\ell, -m} = X_{-k}^{\ell, m}, \quad (154)$$

$$(1 - e^2) X_k^{\ell, m} = X_k^{\ell+1, m} + \frac{e}{2} [X_k^{\ell+1, m-1} + X_k^{\ell+1, m+1}], \quad (155)$$

$$\begin{aligned} \sqrt{1 - e^2} k X_k^{\ell, m} &= m(1 - e^2) X_k^{\ell-2, m} + \frac{e\ell}{2} [X_k^{\ell-1, m-1} - X_k^{\ell-1, m+1}] \\ &= m X_k^{\ell-1, m} + \frac{e}{2} [(m + \ell) X_k^{\ell-1, m-1} + (m - \ell) X_k^{\ell-1, m+1}]. \end{aligned} \quad (156)$$

The first relation (Eq. (154)) allow us to obtain the coefficients $X_k^{-3, -1}$ and $X_k^{-3, -2}$ from the coefficients $X_k^{-3, 1}$ and $X_k^{-3, 2}$, respectively (Table 1). It also allow us to obtain any other coefficient with $m < 0$ from $X_k^{\ell, m}$ with $m > 0$. The second relation (Eq. (155)) with $\ell = -4$ provides

$$\begin{aligned} m = 0 &\Rightarrow (1 - e^2) X_k^{-4, 0} = \frac{e}{2} X_k^{-3, -1} + X_k^{-3, 0} + \frac{e}{2} X_k^{-3, 1}, \\ m = 1 &\Rightarrow (1 - e^2) X_k^{-4, 1} = \frac{e}{2} X_k^{-3, 0} + X_k^{-3, 1} + \frac{e}{2} X_k^{-3, 2}, \\ m = 2 &\Rightarrow (1 - e^2) X_k^{-4, 2} = \frac{e}{2} X_k^{-3, 1} + X_k^{-3, 2} + \frac{e}{2} X_k^{-3, 3}. \end{aligned} \quad (157)$$

Finally, from the last relation (Eq. (156)) with $\ell = -3$ we get

$$\begin{aligned} m = 0 &\Rightarrow \sqrt{1 - e^2} k X_k^{-3, 0} = \frac{3}{2} e (X_k^{-4, 1} - X_k^{-4, -1}), \\ m = 1 &\Rightarrow \sqrt{1 - e^2} k X_k^{-3, 1} = 2e X_k^{-4, 2} + X_k^{-4, 1} - e X_k^{-4, 0}, \\ m = 2 &\Rightarrow \sqrt{1 - e^2} k X_k^{-3, 2} = \frac{5}{2} e X_k^{-4, 3} + 2 X_k^{-4, 2} - \frac{1}{2} e X_k^{-4, 1}. \end{aligned} \quad (158)$$

Using these sets of relations, it is possible to express all Hansen coefficients appearing in this work solely as functions of $X_k^{-3,0}$, $X_k^{-3,1}$, and $X_k^{-3,2}$, using the following sequence:

$$\begin{aligned}
X_k^{-4,3} &= \frac{1}{5e} \left[e X_k^{-4,1} - 4 X_k^{-4,2} + 2\sqrt{1-e^2} k X_k^{-3,2} \right], \\
X_k^{-3,3} &= \frac{1}{e} \left[2(1-e^2) X_k^{-4,2} - 2X_k^{-3,2} - e X_k^{-3,1} \right], \\
X_k^{-4,2} &= \frac{1}{2e} \left[e X_k^{-4,0} - X_k^{-4,1} + \sqrt{1-e^2} k X_k^{-3,1} \right], \\
X_k^{-4,1} &= \frac{1}{1-e^2} \left[\frac{e}{2} X_k^{-3,2} + X_k^{-3,1} + \frac{e}{2} X_k^{-3,0} \right], \\
X_k^{-4,0} &= \frac{1}{1-e^2} \left[\frac{e}{2} X_k^{-3,-1} + X_k^{-3,0} + \frac{e}{2} X_k^{-3,1} \right].
\end{aligned} \tag{159}$$

B Hansen coefficients combinations

We let

$$F_+ = \left(\frac{r}{a}\right)^\ell e^{imv}, \quad \text{and} \quad F_- = \left(\frac{r}{a}\right)^\ell e^{-inv}, \tag{160}$$

with derivatives, respectively,

$$F'_+ = -i \frac{dF_+}{dM} = m\sqrt{1-e^2} \left(\frac{r}{a}\right)^{\ell-2} e^{imv} - e\ell \left(\frac{r}{a}\right)^{\ell-1} \frac{e^{i(m+1)v} - e^{i(m-1)v}}{2\sqrt{1-e^2}}, \tag{161}$$

$$F'_- = i \frac{dF_-}{dM} = n\sqrt{1-e^2} \left(\frac{r}{a}\right)^{\ell-2} e^{-inv} - e\ell \left(\frac{r}{a}\right)^{\ell-1} \frac{e^{-i(n+1)v} - e^{-i(n-1)v}}{2\sqrt{1-e^2}}. \tag{162}$$

Using the definition of the Hansen coefficients (Eq. (48)) we have

$$\langle F_+ F_- \rangle_M = \sum_{k=-\infty}^{+\infty} X_k^{\ell,m} X_k^{\ell,n} = \left\langle \left(\frac{r}{a}\right)^{2\ell} e^{i(m-n)v} \right\rangle_M = X_0^{2\ell, m-n}, \tag{163}$$

$$\begin{aligned}
\langle F'_+ F_- \rangle_M &= \sum_{k=-\infty}^{+\infty} k X_k^{\ell,m} X_k^{\ell,n} \\
&= \left\langle m\sqrt{1-e^2} \left(\frac{r}{a}\right)^{2\ell-2} e^{i(m-n)v} - \frac{e\ell}{2\sqrt{1-e^2}} \left(\frac{r}{a}\right)^{2\ell-1} \left(e^{i(m-n+1)v} - e^{i(m-n-1)v} \right) \right\rangle_M \\
&= m\sqrt{1-e^2} X_0^{2\ell-2, m-n} - \frac{e\ell}{2\sqrt{1-e^2}} \left(X_0^{2\ell-1, m-n+1} - X_0^{2\ell-1, m-n-1} \right) \\
&= \frac{m+n}{2} \sqrt{1-e^2} X_0^{2\ell-2, m-n},
\end{aligned} \tag{164}$$

$$\begin{aligned}
\langle F'_+ F'_- \rangle_M &= \sum_{k=-\infty}^{+\infty} k^2 X_k^{\ell,m} X_k^{\ell,n} \\
&= \left\langle \frac{\ell^2 e^2}{4(1-e^2)} \left(\frac{r}{a}\right)^{2\ell-2} \left(2e^{i(m-n)v} - e^{i(m-n+2)v} - e^{i(m-n-2)v} \right) \right\rangle_M \\
&\quad + \left\langle (m-n)\ell \frac{e}{2} \left(\frac{r}{a}\right)^{2\ell-3} \left(e^{i(m-n+1)v} - e^{i(m-n-1)v} \right) + mn(1-e^2) \left(\frac{r}{a}\right)^{2\ell-4} e^{i(m-n)v} \right\rangle_M \\
&= \frac{\ell^2 e^2}{4(1-e^2)} \left(2X_0^{2\ell-2, m-n} - X_0^{2\ell-2, m-n+2} - X_0^{2\ell-2, m-n-2} \right) \\
&\quad + (m-n)\ell \frac{e}{2} \left(X_0^{2\ell-3, m-n+1} - X_0^{2\ell-3, m-n-1} \right) + mn(1-e^2) X_0^{2\ell-4, m-n} \\
&= \ell^2 \left(2X_0^{2\ell-3, m-n} - X_0^{2\ell-2, m-n} \right) + \left(\frac{\ell(m-n)^2}{2\ell-2} + mn - \ell^2 \right) (1-e^2) X_0^{2\ell-4, m-n},
\end{aligned} \tag{165}$$

where to simplify expression (164) we used equation (156), and to simplify expression (165) we used equations (155) and (156) together with (eg. Giacaglia, 1976):

$$(1 - e^2)^2 X_k^{\ell, m} = \left(1 + \frac{e^2}{2}\right) X_k^{\ell+2, m} + e \left[X_k^{\ell+2, m+1} + X_k^{\ell+2, m-1}\right] + \frac{e^2}{4} \left[X_k^{\ell+2, m+2} + X_k^{\ell+2, m-2}\right]. \quad (166)$$

References

- Adams FC, Bloch AM (2015) On the stability of extrasolar planetary systems and other closely orbiting pairs. *Mon. Not. R. Astron. Soc.* 446:3676–3686, DOI 10.1093/mnras/stu2397, [1411.2859](#)
- Alexander ME (1973) The Weak Friction Approximation and Tidal Evolution in Close Binary Systems. *Astrophys. Space Sci.* 23:459–510, DOI 10.1007/BF00645172
- Andrade ENdC (1910) On the Rigidity of the Earth. *Proc R Soc Lond A* 84:1–12
- Ben Jazia A, Lombard B, Bellis C (2014) Wave propagation in a fractional viscoelastic Andrade medium: diffusive approximation and numerical modeling. *Wave Motion* 51:994–1010, DOI 10.1016/j.wavemoti.2014.03.011, [1312.4820](#)
- Bills BG, Neumann GA, Smith DE, Zuber MT (2005) Improved estimate of tidal dissipation within Mars from MOLA observations of the shadow of Phobos. *Journal of Geophysical Research (Planets)* 110(E7):E07004, DOI 10.1029/2004JE002376
- Boué G, Efroimsky M (2019) Tidal evolution of the Keplerian elements. *Celestial Mechanics and Dynamical Astronomy* 131(7):30, DOI 10.1007/s10569-019-9908-2, [1904.02253](#)
- Boué G, Fabrycky DC (2014) Compact Planetary Systems Perturbed by an Inclined Companion. I. Vectorial Representation of the Secular Model. *Astrophys. J.* 789:110, DOI 10.1088/0004-637X/789/2/110, [1405.7632](#)
- Boué G, Laskar J (2009) Spin axis evolution of two interacting bodies. *Icarus* 201:750–767, DOI 10.1016/j.icarus.2009.02.001
- Boué G, Correia ACM, Laskar J (2016) Complete spin and orbital evolution of close-in bodies using a Maxwell viscoelastic rheology. *Celestial Mechanics and Dynamical Astronomy* 126:31–60, DOI 10.1007/s10569-016-9708-x, [1612.02558](#)
- Boué G, Correia ACM, Laskar J (2019) On tidal theories and the rotation of viscous bodies. In: *EAS Publications Series*, EAS Publications Series, vol 82, pp 91–98, DOI 10.1051/eas/1982009
- Challe A, Laclaverie JJ (1969) Disturbing Function and Analytical Solution of the Problem of the Motion of a Satellite. *Astron. Astrophys.* 3:15
- Correia ACM (2006) The core-mantle friction effect on the secular spin evolution of terrestrial planets. *Earth Planet. Sci. Lett.* 252:398–412, DOI 10.1016/j.epsl.2006.10.007
- Correia ACM (2009) Secular Evolution of a Satellite by Tidal Effect: Application to Triton. *Astrophys. J.* 704:L1–L4, DOI 10.1088/0004-637X/704/1/L1, [0909.4210](#)
- Correia ACM, Laskar J, Farago F, Boué G (2011) Tidal evolution of hierarchical and inclined systems. *Celestial Mechanics and Dynamical Astronomy* 111:105–130, DOI 10.1007/s10569-011-9368-9, [1107.0736](#)
- Correia ACM, Boué G, Laskar J, Rodríguez A (2014) Deformation and tidal evolution of close-in planets and satellites using a Maxwell viscoelastic rheology. *Astron. Astrophys.* 571:A50, DOI 10.1051/0004-6361/201424211, [1411.1860](#)
- Correia ACM, Boué G, Laskar J (2016) Secular and tidal evolution of circumbinary systems. *Celestial Mechanics and Dynamical Astronomy* 126:189–225, DOI 10.1007/s10569-016-9709-9, [1608.03484](#)
- Darwin GH (1879) On the bodily tides of viscous and semi-elastic spheroids and on the ocean tides upon a yielding nucleus. *Philos Trans R Soc London* 170:1–35
- Darwin GH (1880) On the secular change in the elements of a satellite revolving around a tidally distorted planet. *Philos Trans R Soc London* 171:713–891
- Darwin GH (1908) *Scientific Papers*. Cambridge University Press
- Efroimsky M (2012) Bodily tides near spin-orbit resonances. *Celestial Mechanics and Dynamical Astronomy* 112:283–330, DOI 10.1007/s10569-011-9397-4, [1105.6086](#)
- Efroimsky M, Lainey V (2007) Physics of bodily tides in terrestrial planets and the appropriate scales of dynamical evolution. *Journal of Geophysical Research (Planets)* 112:E12003, DOI 10.1029/2007JE002908, [0709.1995](#)
- Efroimsky M, Williams JG (2009) Tidal torques: a critical review of some techniques. *Celestial Mechanics and Dynamical Astronomy* 104:257–289, DOI 10.1007/s10569-009-9204-7, [0803.3299](#)
- Ferraz-Mello S (2013) Tidal synchronization of close-in satellites and exoplanets. A rheophysical approach. *Celestial Mechanics and Dynamical Astronomy* 116:109–140, DOI 10.1007/s10569-013-9482-y, [1204.3957](#)
- Frouard J, Efroimsky M (2018) Precession relaxation of viscoelastic oblate rotators. *Mon. Not. R. Astron. Soc.* 473(1):728–746, DOI 10.1093/mnras/stx2328, [1606.04559](#)
- Gevorgyan Y, Boué G, Ragazzo C, Ruiz LS, Correia ACM (2020) Andrade rheology in time-domain. Application to Enceladus’ dissipation of energy due to forced libration. *Icarus* 343:113610, DOI 10.1016/j.icarus.2019.113610, [1912.09309](#)

- Giacaglia GEO (1976) A Note on Hansen's Coefficients in Satellite Theory. *Celestial Mechanics* 14(4):515–523, DOI 10.1007/BF01229062
- Goldstein H (1950) *Classical mechanics*. Addison-Wesley, Reading
- Henning WG, O'Connell RJ, Sasselov DD (2009) Tidally Heated Terrestrial Exoplanets: Viscoelastic Response Models. *Astrophys. J.* 707:1000–1015, DOI 10.1088/0004-637X/707/2/1000, [0912.1907](#)
- Hughes S (1981) The Computation of Tables of Hansen Coefficients. *Celestial Mechanics* 25:101–107, DOI 10.1007/BF01301812
- Hut P (1980) Stability of tidal equilibrium. *Astron. Astrophys.* 92:167–170
- Kaula WM (1964) Tidal dissipation by solid friction and the resulting orbital evolution. *Rev. Geophys.* 2:661–685
- Lambeck K (1980) *The Earth's Variable Rotation: Geophysical Causes and Consequences*. Cambridge University Press
- Laskar J, Boué G (2010) Explicit expansion of the three-body disturbing function for arbitrary eccentricities and inclinations. *Astron. Astrophys.* 522:A60, DOI 10.1051/0004-6361/201014496, [1008.2947](#)
- Love AEH (1911) *Some Problems of Geodynamics*
- Love AEH (1927) *A Treatise on the Mathematical Theory of Elasticity*. New York: Dover Publications
- Mignard F (1979) The evolution of the lunar orbit revisited. I. *Moon and Planets* 20:301–315
- Munk WH, MacDonald GJF (1960) *The Rotation of the Earth; A Geophysical Discussion*. Cambridge University Press
- Murray CD, Dermott SF (1999) *Solar System Dynamics*. Cambridge University Press
- Ogilvie GI, Lin DNC (2004) Tidal Dissipation in Rotating Giant Planets. *Astrophys. J.* 610:477–509, DOI 10.1086/421454, [arXiv:astro-ph/0310218](#)
- Ogilvie GI, Lin DNC (2007) Tidal Dissipation in Rotating Solar-Type Stars. *Astrophys. J.* 661(2):1180–1191, DOI 10.1086/515435, [astro-ph/0702492](#)
- Peltier WR (1974) The impulse response of a Maxwell earth. *Reviews of Geophysics and Space Physics* 12:649–669, DOI 10.1029/RG012i004p00649
- Remus F, Mathis S, Zahn JP, Lainey V (2012) Anelastic tidal dissipation in multi-layer planets. *Astron. Astrophys.* 541:A165, DOI 10.1051/0004-6361/201118595, [1204.1468](#)
- Renaud JP, Henning WG (2018) Increased Tidal Dissipation Using Advanced Rheological Models: Implications for Io and Tidally Active Exoplanets. *Astrophys. J.* 857(2):98, DOI 10.3847/1538-4357/aab784, [1707.06701](#)
- Rochester MG, Smylie DE (1974) On changes in the trace of the earth's inertia tensor. *J. Geophys. Res.* 79:4948–4951, DOI 10.1029/JB079i032p04948
- Singer SF (1968) The Origin of the Moon and Geophysical Consequences. *Geophys. J. R. Astron. Soc.* 15:205–226
- Taylor PA, Margot JL (2010) Tidal evolution of close binary asteroid systems. *Celestial Mechanics and Dynamical Astronomy* 108(4):315–338, DOI 10.1007/s10569-010-9308-0, [1101.1500](#)